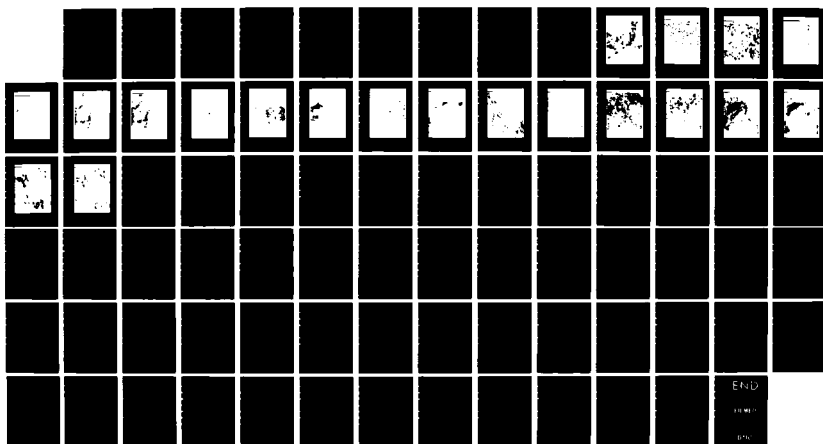


AD-A161 688 SPECTRAL IMAGING WITH A CID CAMERA(U) LOCKHEE MISSILES 1/1  
RAND SPACE CO INC PALO ALTO CA T D TARBELL 22 MAR 85  
LMSC/F059543 AFGL-TR-85-0075 F19228-82-C-0030

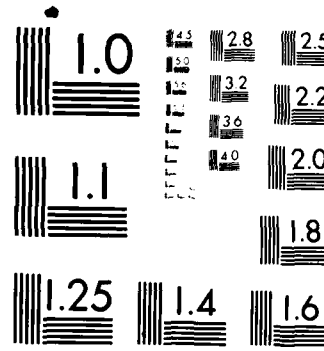
UNCLASSIFIED

F/G 3/2

NL



END  
EVEN  
BPC



MICROCOPY RESOLUTION TEST CHART  
NATIONAL BUREAU OF STANDARDS 16 x A

AD-A161 608

AFGL-TR-85-0075

(12)

SPECTRAL IMAGING WITH A CID CAMERA

Theodore D. Tarbell

Lockheed Missiles & Space Co., Inc.  
3251 Hanover Street  
Palo Alto, CA 94304

Final Report  
4 February 1982 - 14 September 1984

22 March 1985

DTIC FILE COPY

Approved for public release; distribution unlimited

4

07 26 1985

D

AIR FORCE GEOPHYSICS LABORATORY  
AIR FORCE SYSTEMS COMMAND  
UNITED STATES AIR FORCE  
HANSOM AFB, MASSACHUSETTS 01731

A

11 20-85 028

"This technical report has been reviewed and is approved for publication."

Stephen L. Keil

STEPHEN L. KEIL  
Contract Manager

Rita C. Sagalyn

RITA C. SAGALYN  
Division Director

This report has been reviewed by the ESD Public Affairs Office (PA) and is releasable to the National Technical Information Service (NTIS).

Qualified requestors may obtain additional copies from the Defense Technical Information Center. All others should apply to the National Technical Information Service.

If your address has changed, or if you wish to be removed from the mailing list, or if the addressee is no longer employed by your organization, please notify AFGL/DAA, Hanscom AFB, MA 01731. This will assist us in maintaining a current mailing list.

UNCLASSIFIED

SECURITY CLASSIFICATION OF THIS PAGE

AD-A161 608

## REPORT DOCUMENTATION PAGE

1a. REPORT SECURITY CLASSIFICATION Unclassified		1b. RESTRICTIVE MARKINGS	
2a. SECURITY CLASSIFICATION AUTHORITY		3. DISTRIBUTION/AVAILABILITY OF REPORT Approved for public release; distribution unlimited	
2b. DECLASSIFICATION/DOWNGRADING SCHEDULE			
4 PERFORMING ORGANIZATION REPORT NUMBER(S) LMSC/F059543		5. MONITORING ORGANIZATION REPORT NUMBER(S) AFGL-85-0075	
6a. NAME OF PERFORMING ORGANIZATION Lockheed Missiles & Space Co., Inc.	6b. OFFICE SYMBOL (If applicable) Dept. 91-30	7a. NAME OF MONITORING ORGANIZATION Air Force Geophysics Laboratory	
6c. ADDRESS (City, State and ZIP Code) 3251 Hanover Street Palo Alto, CA 94304	7b. ADDRESS (City, State and ZIP Code) Hanscom AFB, MA 01731 Monitor: Dr. S. L. Keil/PHS		
8a. NAME OF FUNDING/SPONSORING ORGANIZATION AFGL	8b. OFFICE SYMBOL (If applicable) PHS	9. PROCUREMENT INSTRUMENT IDENTIFICATION NUMBER F19628-82-C-0030	
8c. ADDRESS (City, State and ZIP Code) Hanscom AFB, MA 01731	10. SOURCE OF FUNDING NOS.		
11. TITLE (Include Security Classification) SPECTRAL IMAGING WITH A CID CAMERA (Unclassified)	PROGRAM ELEMENT NO. 61102F	PROJECT NO. 2311	TASK NO. G3
12. PERSONAL AUTHOR(S) Theodore D. Tarbell	WORK UNIT NO. C14		
13a. TYPE OF REPORT Final Report	13b. TIME COVERED FROM 2/4/82 TO 9/14/84	14. DATE OF REPORT (Yr., Mo., Day) 1985 March 22	15. PAGE COUNT 84
16. SUPPLEMENTARY NOTATION			
17. COSATI CODES	18. SUBJECT TERMS (Continue on reverse if necessary and identify by block number) spectral imaging; CID camera; tunable filters; solar physics; magnetohydrodynamics; image processing		
19. ABSTRACT (Continue on reverse if necessary and identify by block number) This report describes a program of spectral imaging observations of the solar atmosphere using the Sacramento Peak Vacuum Tower Telescope. The observations were obtained with Lockheed instruments including: an active tilt mirror for image motion compensation; polarization analyzer; narrowband tunable birefringent filter; photoelectric CID array camera; digital video image processor; and a microcomputer controller. Five observing runs were made, three of them with the entire system in operation. The images obtained were processed to measure magnetic and velocity fields in the solar photosphere with very high spatial resolution - 0.5 arcseconds on the best frames. Sets of these images have been studied to address three scientific problems: (1) the relationship among small magnetic flux tubes, downdrafts and granulation; (2) the puzzling flux changes in isolated magnetic features in a decaying active region; (3) the temporal power spectrum of the magnetogram signal in isolated flux tubes. Examples of the narrowband images are included in the report, along with abstracts and manuscripts of papers resulting from this research.			
20. DISTRIBUTION/AVAILABILITY OF ABSTRACT UNCLASSIFIED/UNLIMITED <input checked="" type="checkbox"/> SAME AS RPT. <input type="checkbox"/> DTIC USERS <input type="checkbox"/>		21. ABSTRACT SECURITY CLASSIFICATION Unclassified	
22a. NAME OF RESPONSIBLE INDIVIDUAL S. L. Keil		22b. TELEPHONE NUMBER (Include Area Code)	22c. OFFICE SYMBOL PHS

## SUMMARY

Lockheed Missiles and Space Company, Incorporated, has performed a program of spectral imaging observations of the solar atmosphere using the Sacramento Peak Vacuum Tower Telescope. The observations were obtained with Lockheed instruments including: an active tilt mirror for image motion compensation; polarization analyzer; narrowband tunable birefringent filter; photoelectric CID array camera; digital video image processor; and a microcomputer controller. Five observing runs were made, three of them with the entire system in operation. The images obtained were processed to measure magnetic and velocity fields in the solar photosphere with very high spatial resolution - 0.5 arcseconds on the best frames. Sets of these images have been studied to address three scientific problems: (1) the relationship among small magnetic flux tubes, downdrafts and granulation; (2) the puzzling flux changes in isolated magnetic features in a decaying active region; (3) the temporal power spectrum of the magnetogram signal in isolated flux tubes. Examples of the narrowband images are included in the report, along with abstracts and manuscripts of papers resulting from this research.



## BACKGROUND

Lockheed Missiles and Space Company, Incorporated, has carried out a program of spectral imaging observations of the solar atmosphere, using the Sacramento Peak Vacuum Tower Telescope. All components for a sensitive photoelectric spectral imaging system were assembled, utilizing previous developments sponsored by Air Force, NASA, and Lockheed Independent Research funds. These instruments were used to study convective flows, hydrodynamic wave modes and magnetic flux tubes on the sun with high accuracy and resolution. Previous observations by Lockheed personnel had concentrated on studying the three-dimensional structure of magnetic fields in the photosphere and chromosphere and on learning the most informative diagnostic techniques which are possible with tunable, narrow-band filter observations. This work had revealed a rich variety of phenomena which could be studied by spectral imaging. However, the time dependence and dynamics had not been addressed in any detail because of the lack of an automatic filter control system and the data handling problem with large-volume film and video recording of raw data. Over the past five years, we acquired the components of an automated digital system, largely as engineering models for flight hardware of the Spacelab 2 Solar Optical Universal Polarimeter. Specifically, we operated an image motion compensation system, polarization analyzer, tunable filter, photoelectric CID array camera, digital video image processor and microcomputer controller. The video processor derived images of brightness, velocity and magnetic fields from raw CID frames and made video movies of these processed images. These data were analyzed using the image processing systems at Lockheed and at Sacramento Peak.

## INSTRUMENTATION

The major components of the spectral imaging system are briefly described in this section. Conceptually, these comprise an engineering model of the Lockheed Solar Optical Universal Polarimeter (SOUP), which will fly on the shuttle flight Spacelab 2 in the summer of 1985. The SOUP instrument is a much more powerful observing tool, and the engineering models have only once played together to simulate its operation, in October, 1984. Nevertheless, the engineering models represent a substantial investment of effort and funds, and they have obtained unique and exciting solar observations to date. Subsets of them will continue to observe the sun periodically.

**Tunable Filter:** This is a Lyot-type birefringent filter with a 75 mÅ band-pass at 5250 Å. It can be tuned to any wavelength between 5000 and 6600 Å, provided an 8 Å blocker is available. A HeNe laser provides wavelength calibration, accurate to a few mÅ. Once solar line positions are stored initially, they can be recalled with arbitrary offsets from line center, again, accurate to a few mÅ. Optically, the filter is of good quality, as evidenced by the very sharp images (0.4 - 0.6 arcsecond resolution) obtained with it since 1979.

**Prefilters:** A wheel containing six waveplates provides polarization analysis in right or left circular and four linear polarizations. An identical wheel containing dielectric interference filters blocks the spectrum, passing one of eight regions centered on 5173, 5250, 5576, 5876, 5896, 6302, 6328 or 6563.

**Image Motion Compensation:** An agile tilt mirror located at a telescope pupil stabilizes the image despite atmospheric wander and telescope shake. It has piezoelectric transducers for speed, a simple integrator controller, and a quad cell centering an image of a sunspot to provide the error signal. When operated properly, the system stabilizes the image of the sunspot (or the mean position of a spot much larger than an isoplanatic patch) to a small fraction of the seeing disk.

**CID Camera:** This SOUP engineering model uses a GE CID-11B array image sensor. It has 248 x 244 pixels of 46 x 35 microns each. It can be read out non-destructively in 0.5 seconds, digitized to 12 bits. The best sensors can attain signal-to-noise ratios of 500-1000 and are linear to a fraction of a percent (after a weak pre-exposure flash of light). Fixed-pattern gain variations show a checkerboard pattern at the 5% level. In nearly-collimated monochromatic light, large, smoothly-varying fringes are seen at the 20% level. Both of these patterns cancel out to a fraction of a percent in magnetograms, which are ratios of an image difference to an image sum. Thus, real-time, relative differential photometry of high sensitivity can be done. The camera was originally built by R. Aikens of Photometrics, Ltd., of Tucson, using designs developed at Kitt Peak National Observatory.

**Digital Video Processor:** This is a partial duplicate of the SOUP on-board image processor. It receives digital frames from the CID camera, performs arithmetic for gain, offset and ratio corrections on three full-frame memories, and displays two images simultaneously on separate video channels. A low-speed parallel interface to the microcomputer is used for commands and (limited) data transfer: passing a full frame to the microcomputer and storing it on disk takes about 30 seconds. Therefore, videotape or videodisk are the preferred storage media.

**Microcomputer Controller:** The computer is a DEC LSI 11-23, mounted in a VT-100 terminal. It runs the RSX-11M operating system with a Winchester disk (8 megabytes) for storage. The computer controls all hardware through DR11C parallel interfaces to the tunable filter electronics box. Early versions of the software were written in assembler language. However, in 1984, a modular Fortran version was written which controls the tunable filter, prefilters, film and/or CID cameras, video processor and video disk recorder. New scientific observing sequences can be entered at a fairly high level, a vast improvement over the previous assembler code.

#### OBSERVATIONS

The first observing run took place in late October and early November of 1982. Since a film camera was used in place of the CID camera, it was primarily supported by other funds. The LSI-11 computer orchestrated the tunable filter, prefilters and 35-mm Acme camera in a complex observing program covering four solar lines: Fe I 5250 and 5576, Mg I 5173 and H-alpha. Two days of very good seeing were spent on a rapidly growing active region near disk center. Approximately 150 of these frames have been digitized using the SPO fast microphtometer. Some examples are included in Appendix A.

In January, 1983, a second observing run was made to test the Lockheed active mirror system of Dr. R. Smithson. No spectral imaging was attempted. We

concluded that the active mirror was too new and complex to try a joint observing run with both instrument systems in 1983.

The entire spectral imaging system was operated at the Tower Telescope in November, 1983. An integrated control program made a continuous series of magnetograms and intensity frames in the blue wing of Fe I 6302. These were displayed on video monitors by the image processor and recorded on video-cassettes. Simultaneously, Dr. Luc Dame of LSPS, France, recorded K line images with a Lockheed filter and the SPO CCD camera. Synchronized movies of the K line and magnetograms with a cycle time of 12 seconds were obtained for about 20 minutes in good seeing. Later in November, about 30 of the best magnetograms were digitized from the videotape. A representative sample of the digital CID frames was also saved on the Winchester disk.

The fourth observing run, in December, 1983, was a repeat of the November experiment. Two hours of data in fairly good seeing was obtained. A short gap occurred every 20 minutes or so for a tunable filter calibration. The video digitizer at Big Bear Solar Observatory has been used to obtain 240 magnetograms in digital FITS files on tape. These data have not yet been analyzed; they are being sent to Dr. Dame for power spectral analysis and comparison with the K line time series.

In September and October, 1984, a fifth observing run took place, supported by other funds. This represented the first serious attempt to operate the tunable filter system in the compensated image formed by the Lockheed active mirror. Unfortunately, this attempt was frustrated by bad weather in the first week of the observing run. In the second week, the complete spectral imaging system was run in a training exercise for the Spacelab 2 payload crew. The microcomputer was programmed to run 15 different observing sequences simulating the SL2 SOUP instrument. Only one day of fair seeing occurred. The data was videotaped but is not worth analyzing from a scientific point of view.

#### ACKNOWLEDGEMENTS

Many skilled people at Lockheed and at Sacramento Peak have made this research possible by their contributions. The Tower staff of Horst Mauter, Dick Mann, Fritz Stauffer, Larry Wilkins and Ray Smartt have spared no effort to make our visits successful. Larry November and Steve Keil have also provided essential help with data analysis at Sacramento Peak. The observational skill of Harry Ramsey is largely responsible for the quality of our best runs. Chris Edwards, Ken Topka, Mike Levay, Bob Smithson, Ron Sharbaugh, Luc Dame and Alan Title have also put in very long days at the telescope, striving for a flawless run during the 30 minutes of good seeing. In Palo Alto, the instruments have been built and debugged by a large team, including Ralph Reeves, Gary Kelly, Mike Finch, Al Pelayo, Bill Rosenberg, Steve Schoolman and Ray Bellantoni. Our summer students, especially Stuart Ferguson and Chris Rhode, have written many of the computer programs for the image displays. The generous support of Lockheed management via the Independent Research Fund has provided much of the instrumentation.

## APPENDIX A

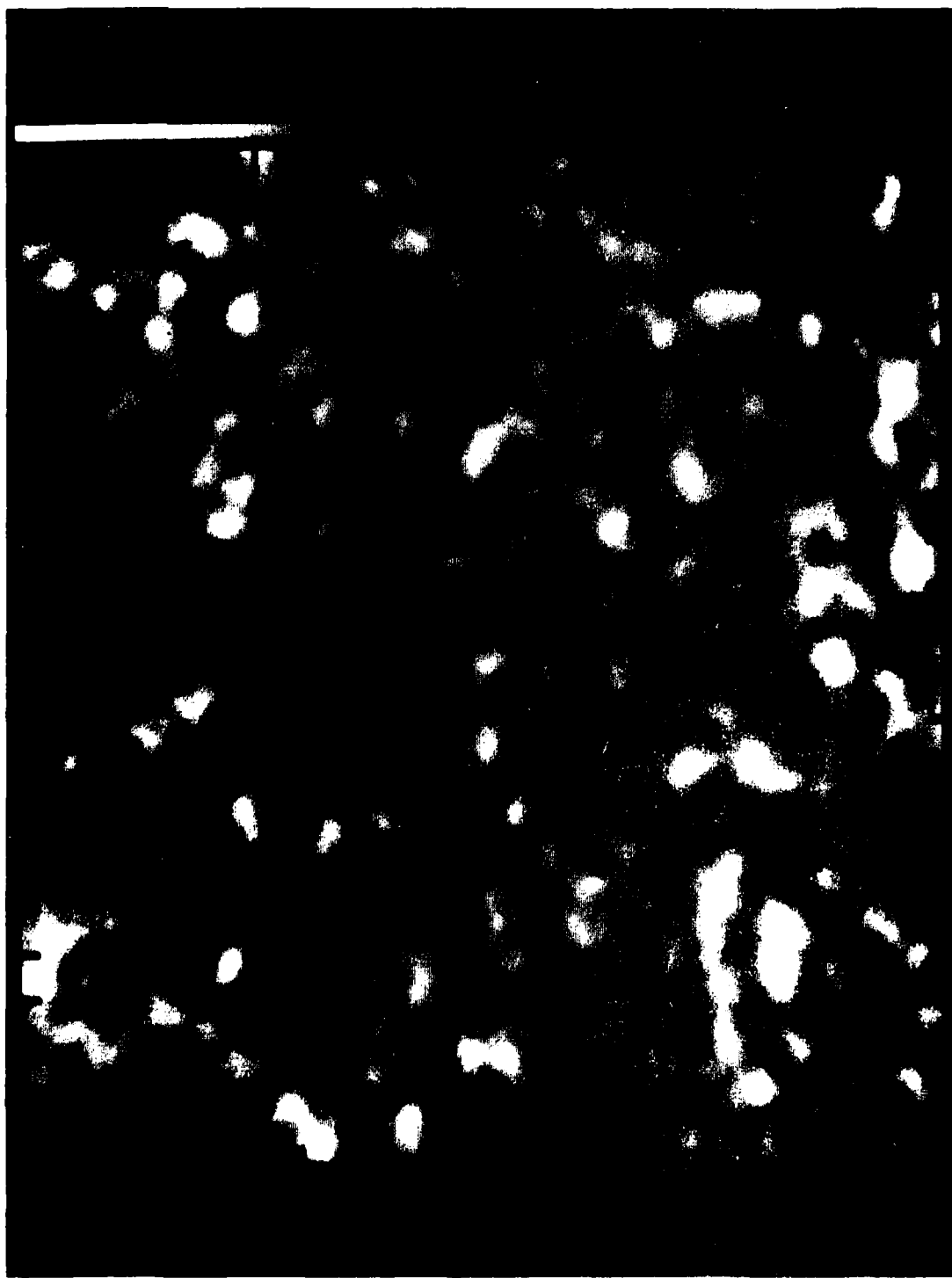
Examples of the narrowband solar images obtained under this contract are presented here. All of these prints were copied from the video of the Grinnell GMR-274 digital image display at Lockheed. A Tektronix 4634 Image Forming Module was used for quick, medium-quality, gray-scale prints. Black and white glossies, color prints (pseudo-color renditions) and slides can also be made on request using a Videoprint 5000 camera. Several different routes have led from the telescope to the Grinnell. Film frames (Kodak 2415) have been developed at SPO and digitized with the SPO Fast Microphotometer or the Lockheed PDS 1010G. A few digital frames were stored on Winchester disk from the video processor. Video magnetograms recorded on Betamax cassettes from the video processor have been digitized at Big Bear Solar Observatory. Many of these images were created in the Lockheed VAX or PDP 11 computers from raw intensity frames.



Magnetogram of a unipolar plage in a young active region near disk center. Tick marks are 2 arcseconds; field-of-view is approximately  $50 \times 50$  arcseconds. The paper on page B-4 is based on analysis of this region, which was observed in the line Fe I 5250.2.



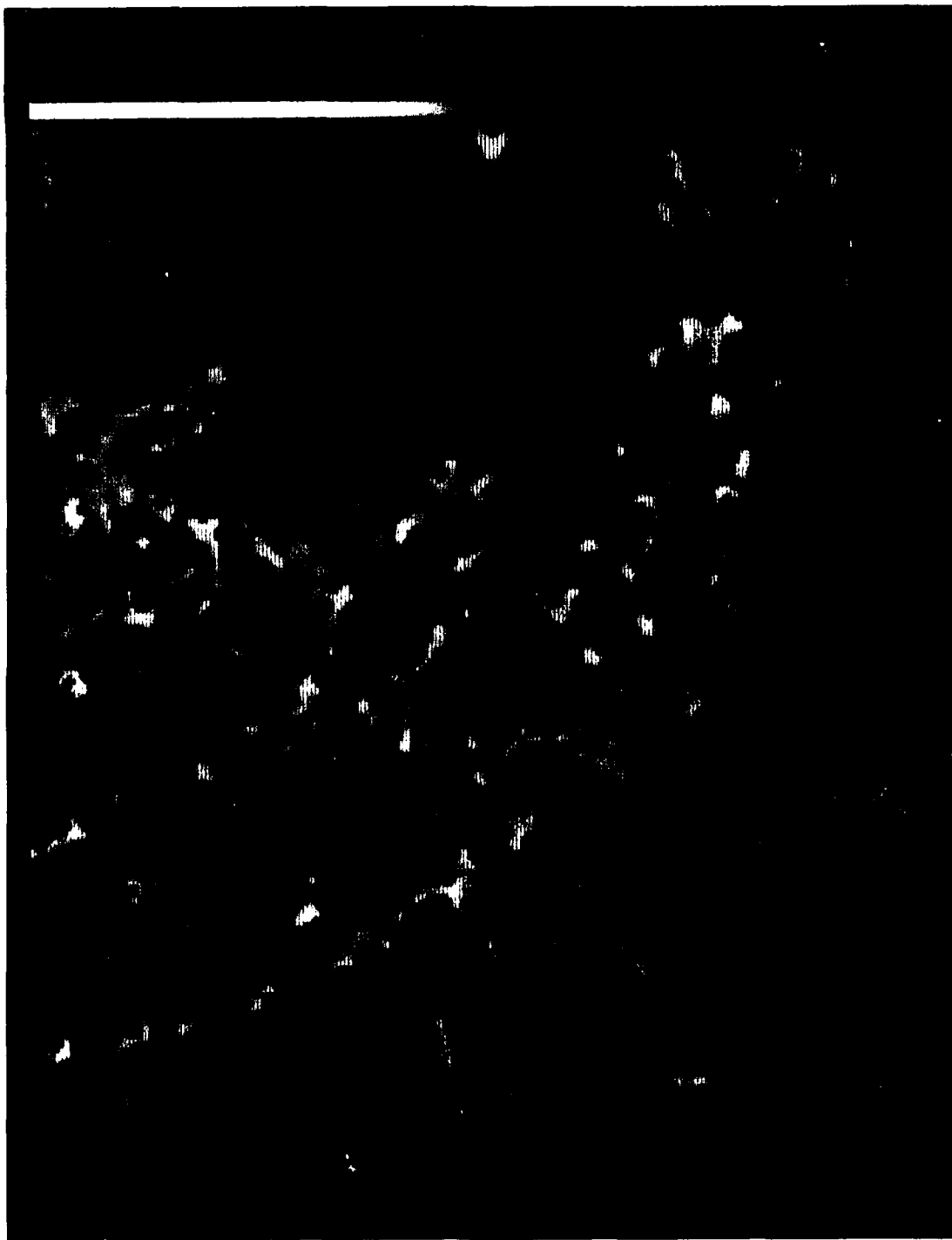
Continuum image (near 5250) of the same region.  
Three pores and much abnormal granulation are  
present. All views of this region are coaligned  
to about 0.25 arcseconds.



Velocity in the wings of 5250, at about  $\pm 50$  mA for the same region. Upflow is light, downflow is dark. The zero point is taken to be the average over the whole frame.



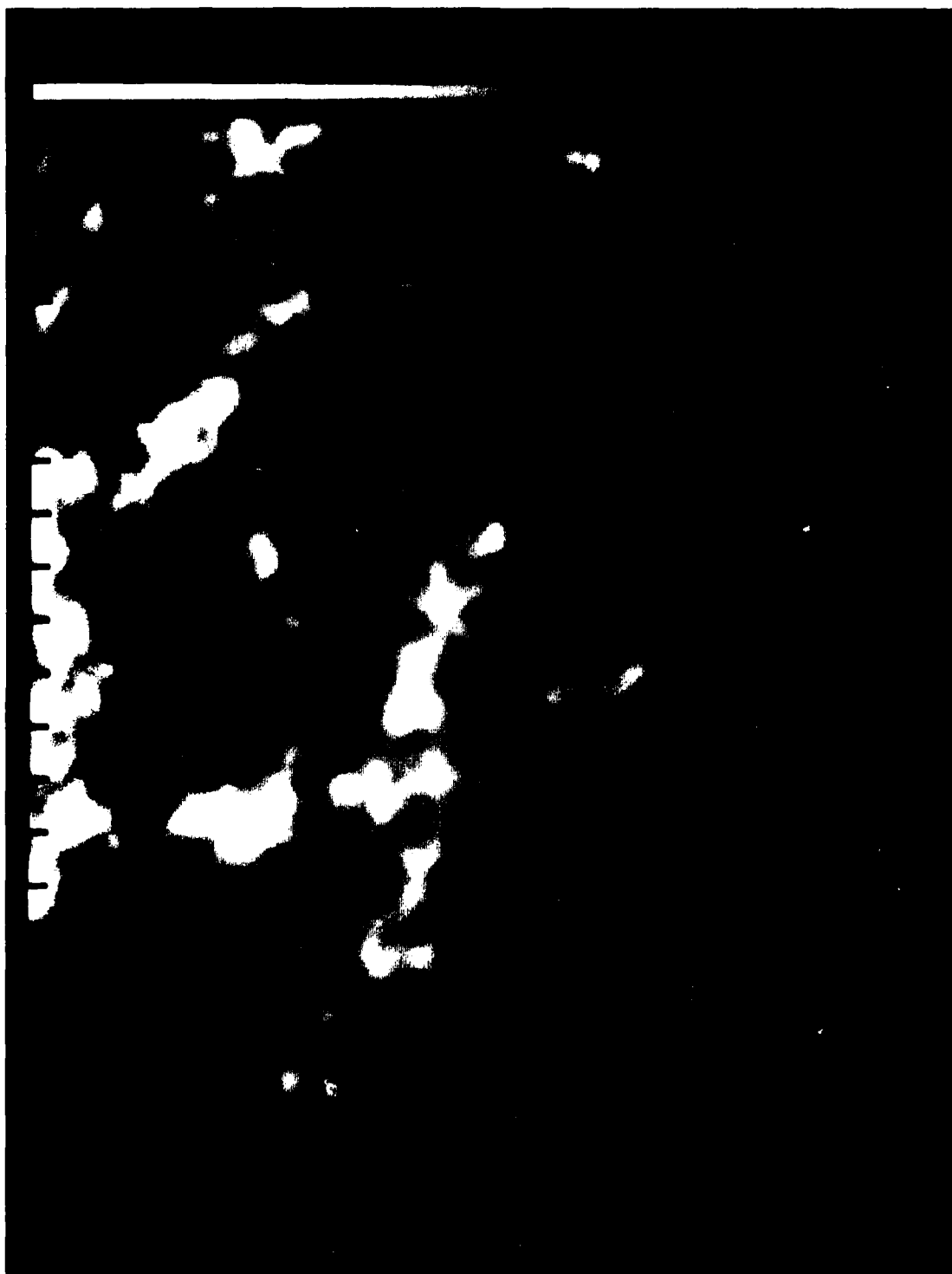
Overlay of the locus of strong magnetic fields on the Dopplergram (dark = downflow). Magnetic flux tubes tend to occur in downflow lanes.



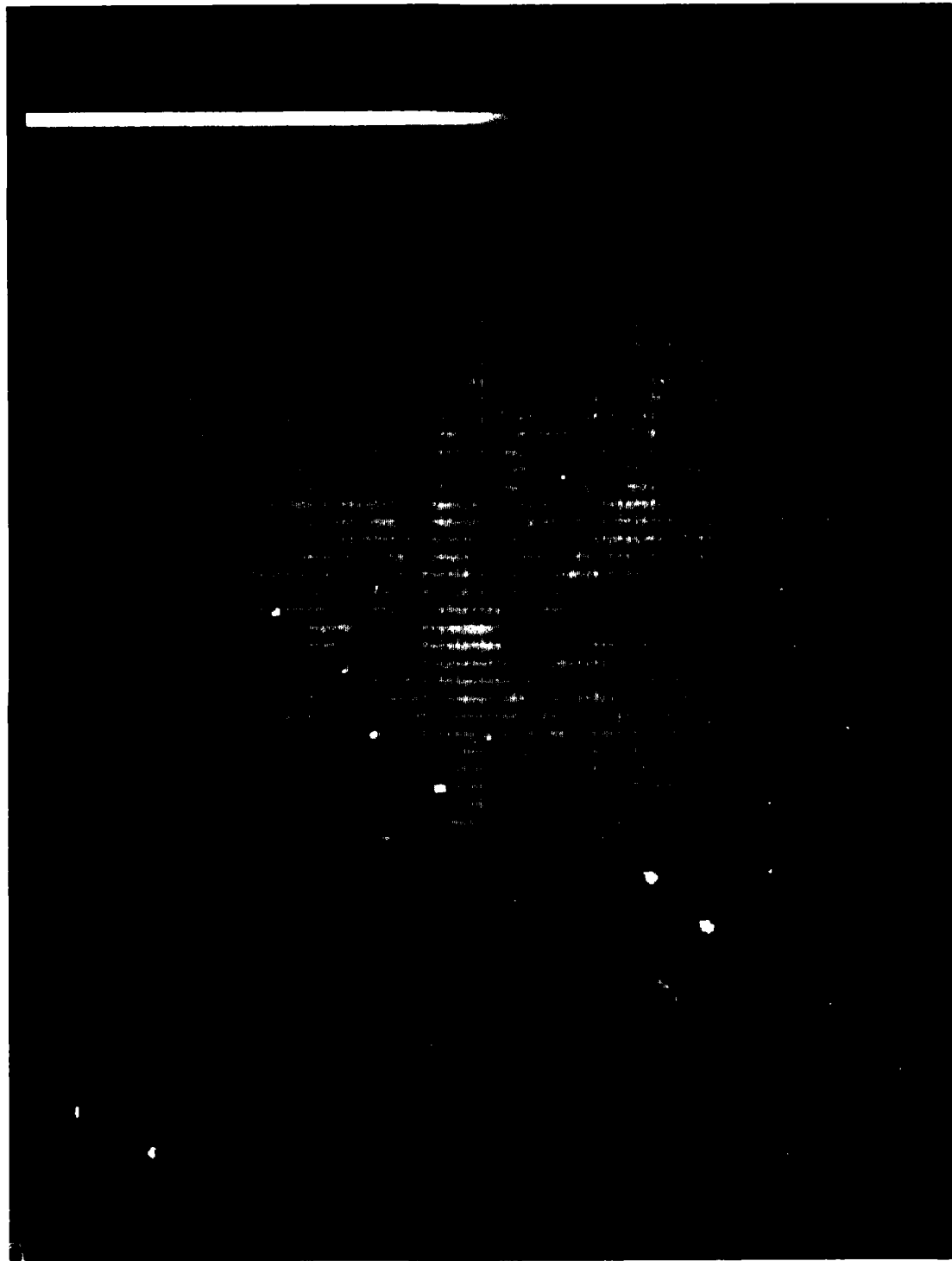
Overlay of the locus of strong magnetic fields on the continuum image. The correlation with the dark lanes is present in some areas of the picture but is not nearly as clear as on the velocity image.



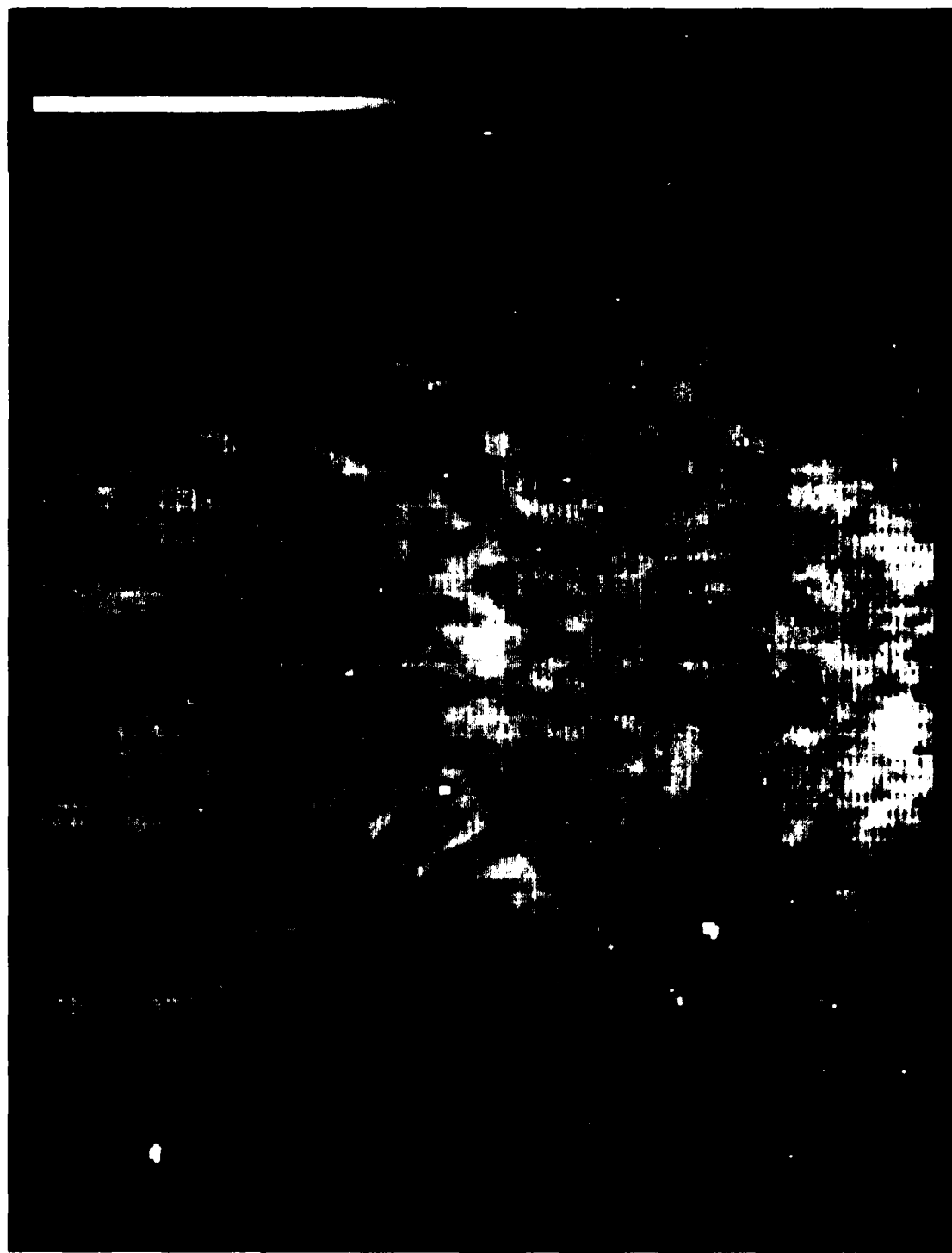
Magnetogram in Fe I 6302 made with the CID camera and video processor on the November, 1983, observing run. This frame was digitized from videotape. It shows the best seeing obtained in any run with the CID camera. Tick marks are 5 arcseconds.



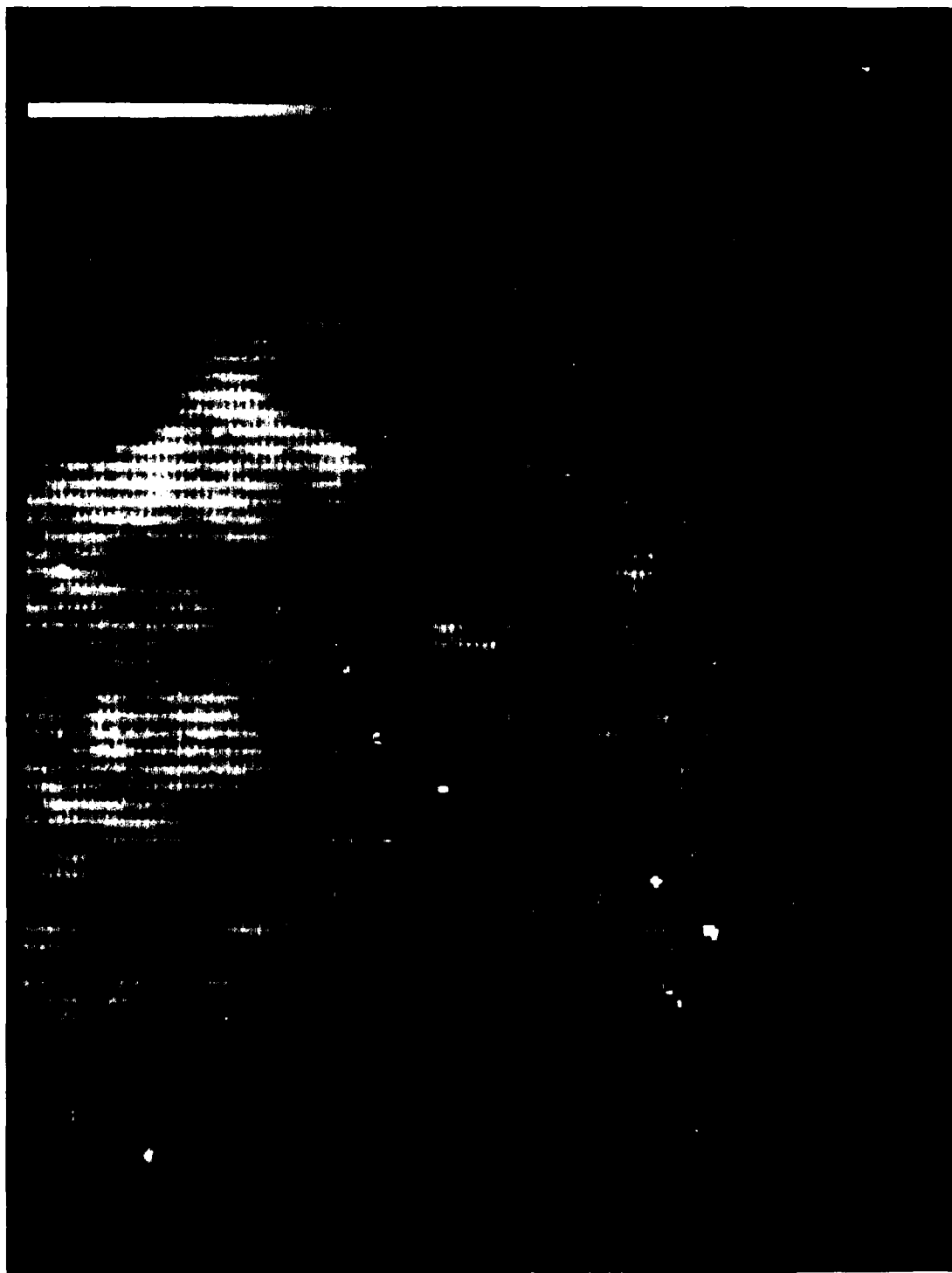
Magnetogram made 18 minutes before the previous one. Very few changes in network fragments are seen at this resolution; some of the features inside the large cell may have changed. According to Dame, these correspond to "K-grains" in the Ca II K line.



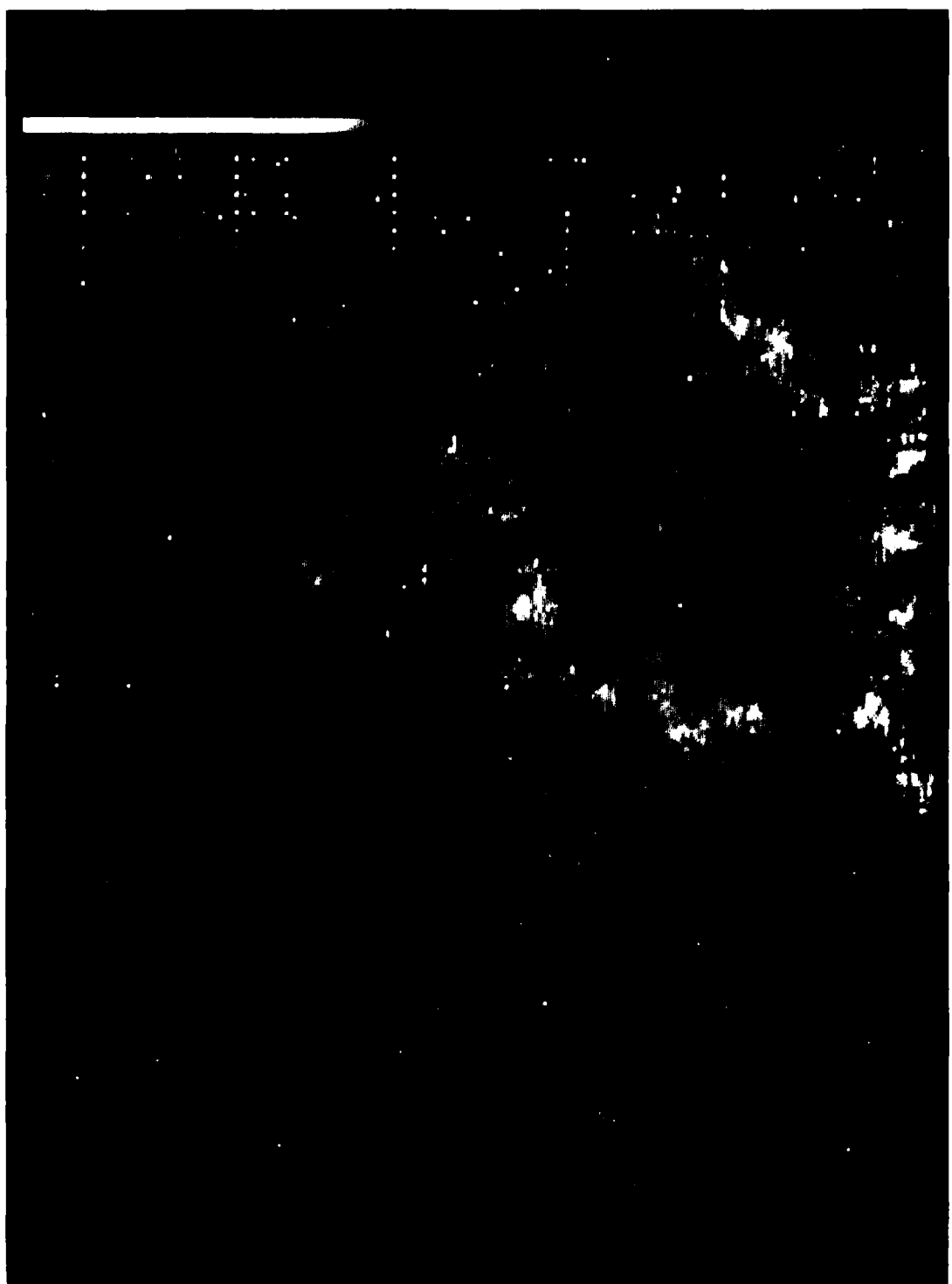
CID image of the same region at 6302.5 line center. This frame was stored digitally on the Winchester disk. No gain correction has been done. Most of this fixed pattern noise is absent in the magnetograms, but it was difficult to remove from the intensity frames.



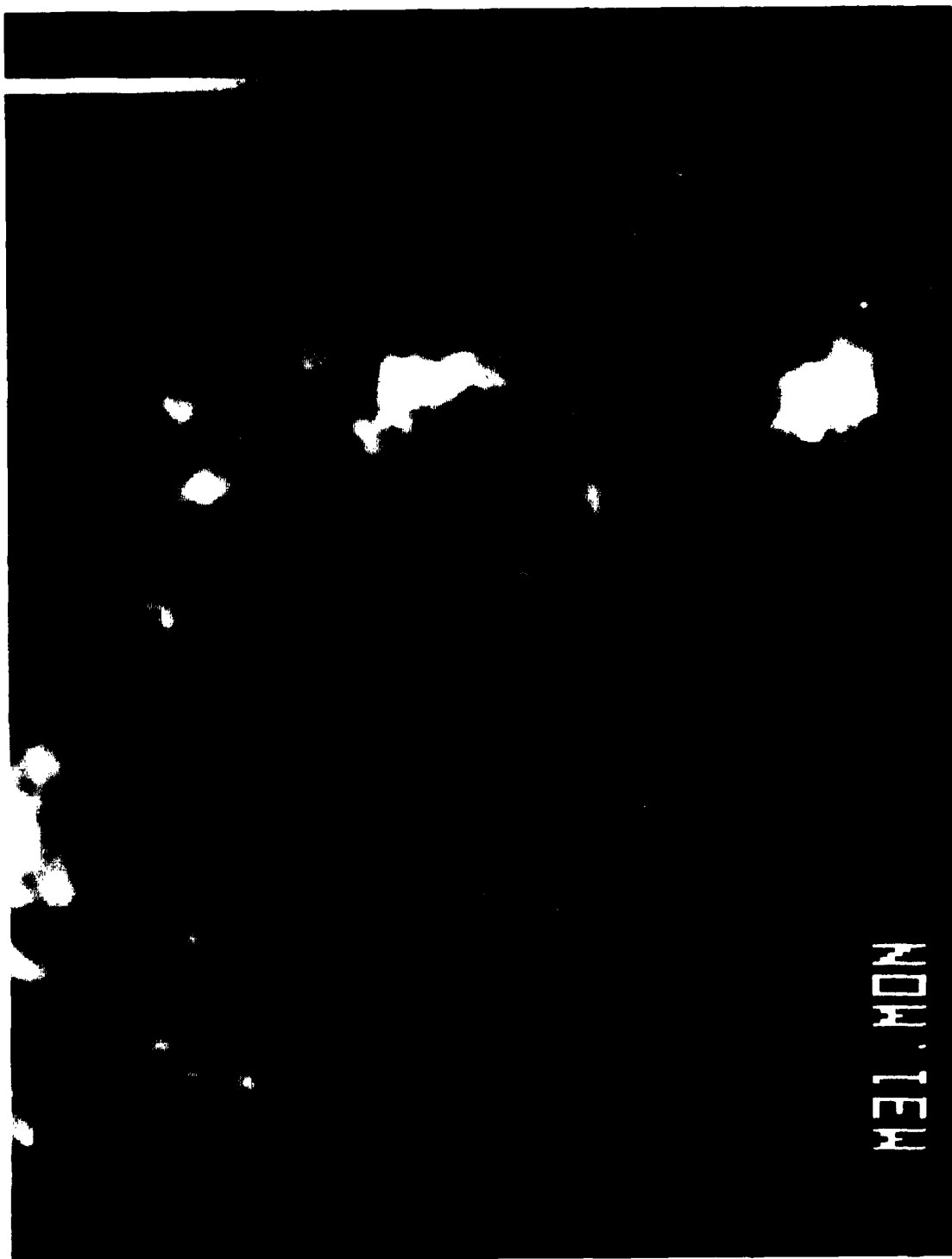
CID frame of the same region at H-alpha line center.



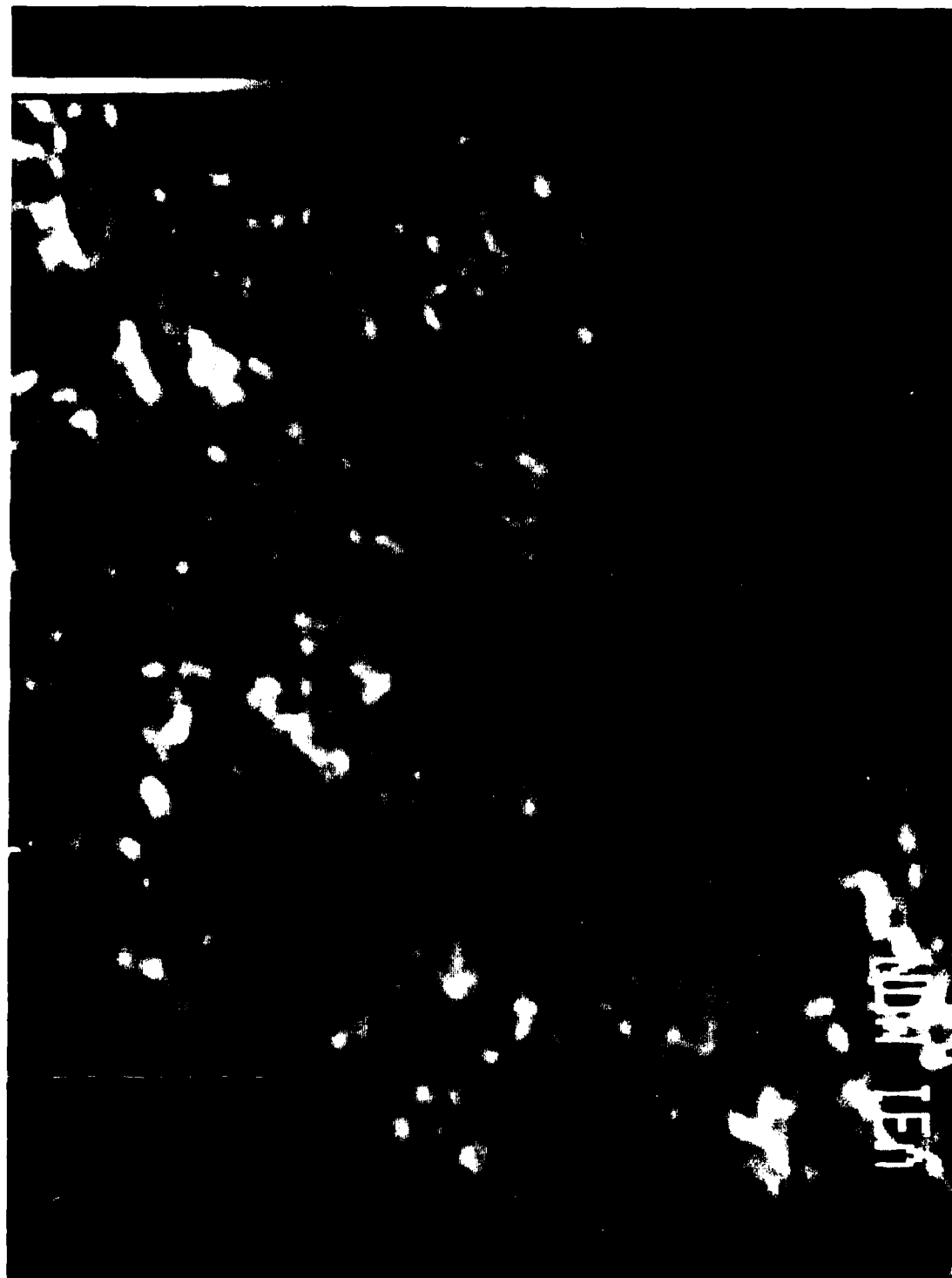
CID frame of the same region in the red wing of H-alpha.



**Magnetogram** of the same region, in somewhat worse seeing than the previous ones. This frame was stored digitally on the Winchester disk. Variations in the checkerboard noise pattern of the device cause the bad pixels on the right side.



Magnetogram of a growing active region near disk center from the October, 1982, observing run. Tick marks are 5 arcseconds. Frames spanning 2.5 hours have been studied, showing several emerging bipoles of flux in the right-center part of the picture. Fe I 5250.2 was used.



Doppler image of the same region, made at  $\pm 50$  mA in 5250. Note the lack of flow in the sunspots, except for some Evershed flow in the penumbrae. In this region, the magnetic-downflow correlation is just a slight statistical preference.



Continuum image of the same region. This is first of a series of frames showing the height coverage possible with the tunable filter.

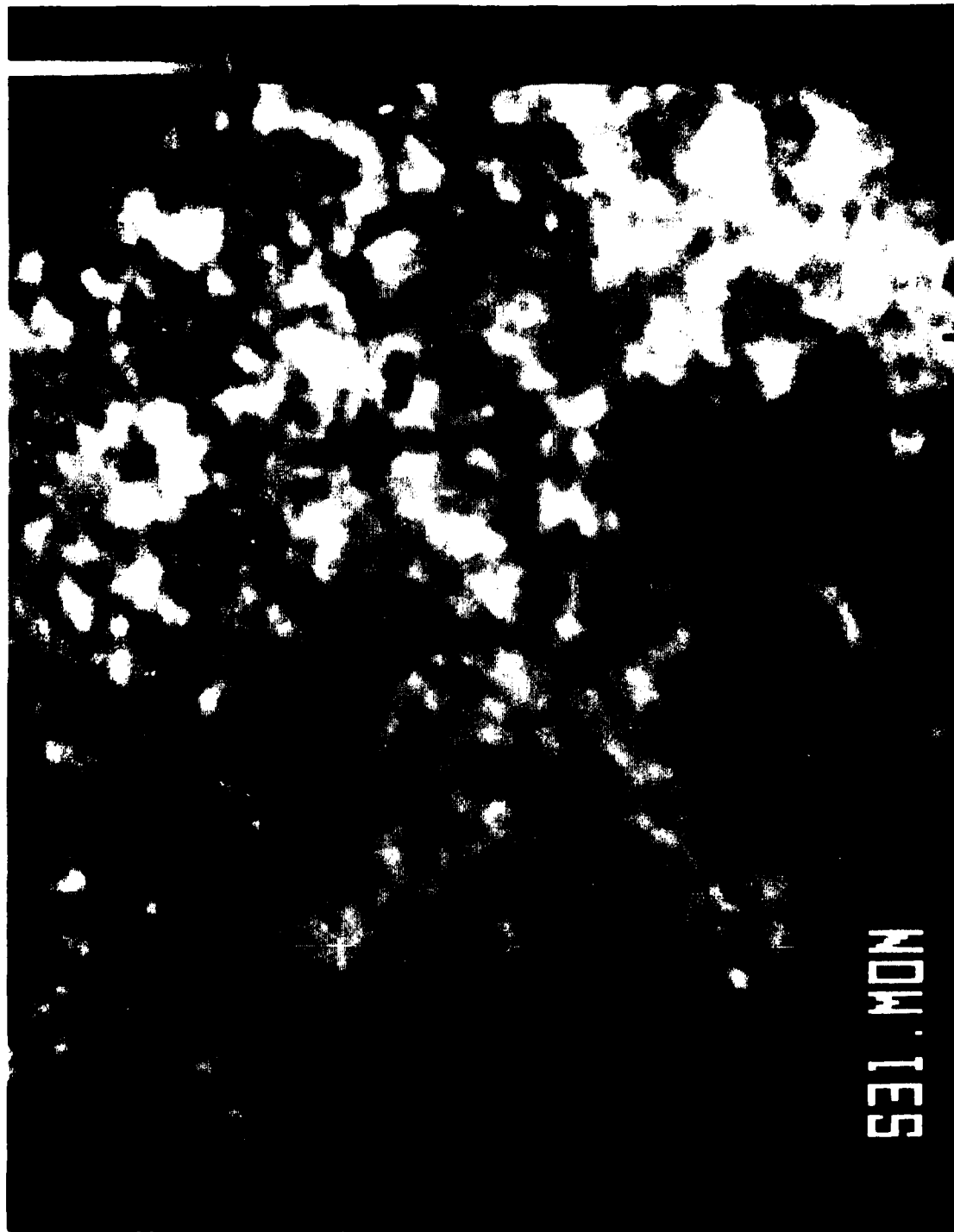


Image of the same region in the blue wing of 5250,  
showing the middle photosphere.

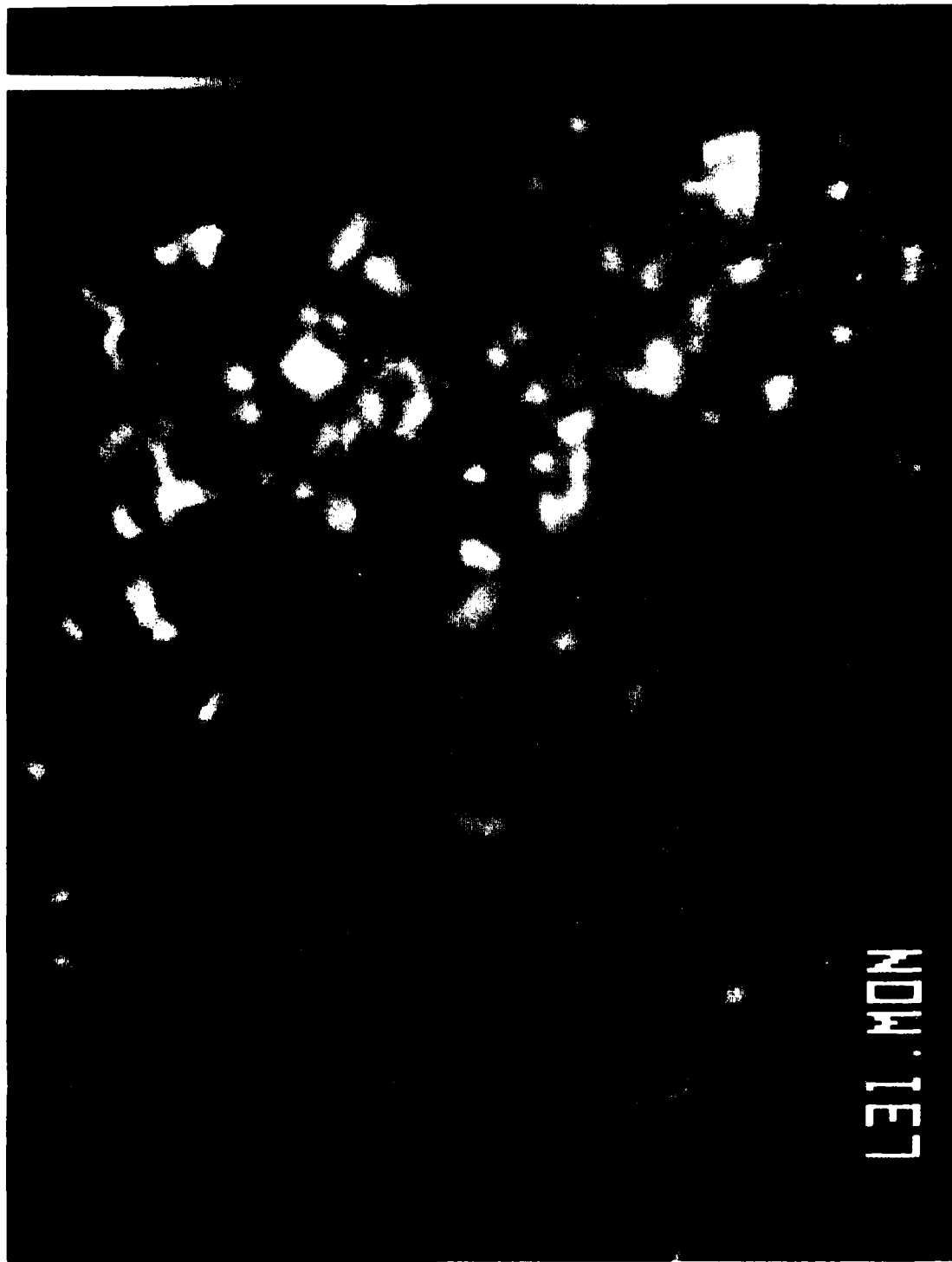


Image of the same region in the blue wing of Mg I 5173, showing the upper photosphere near the temperature minimum.

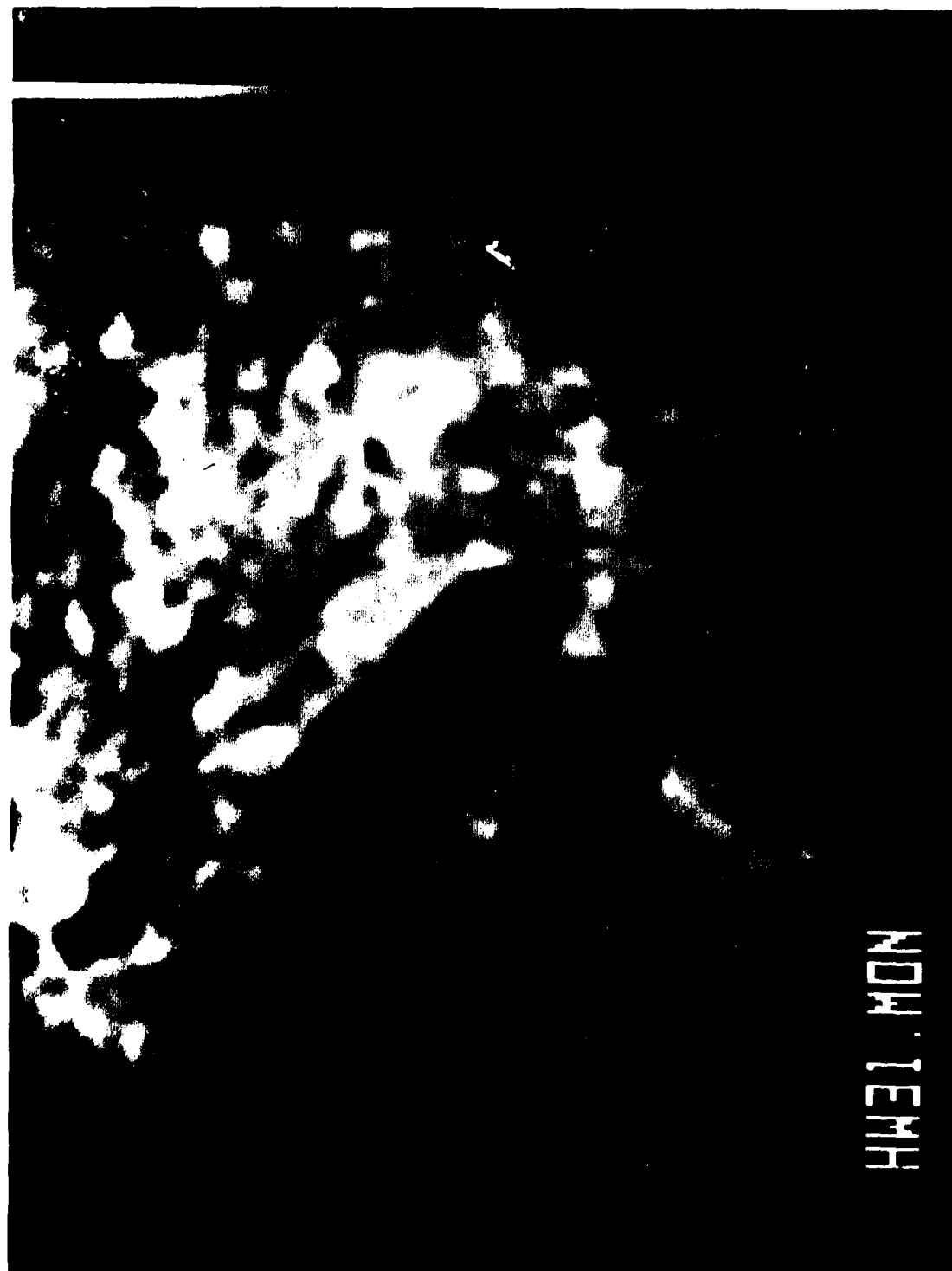
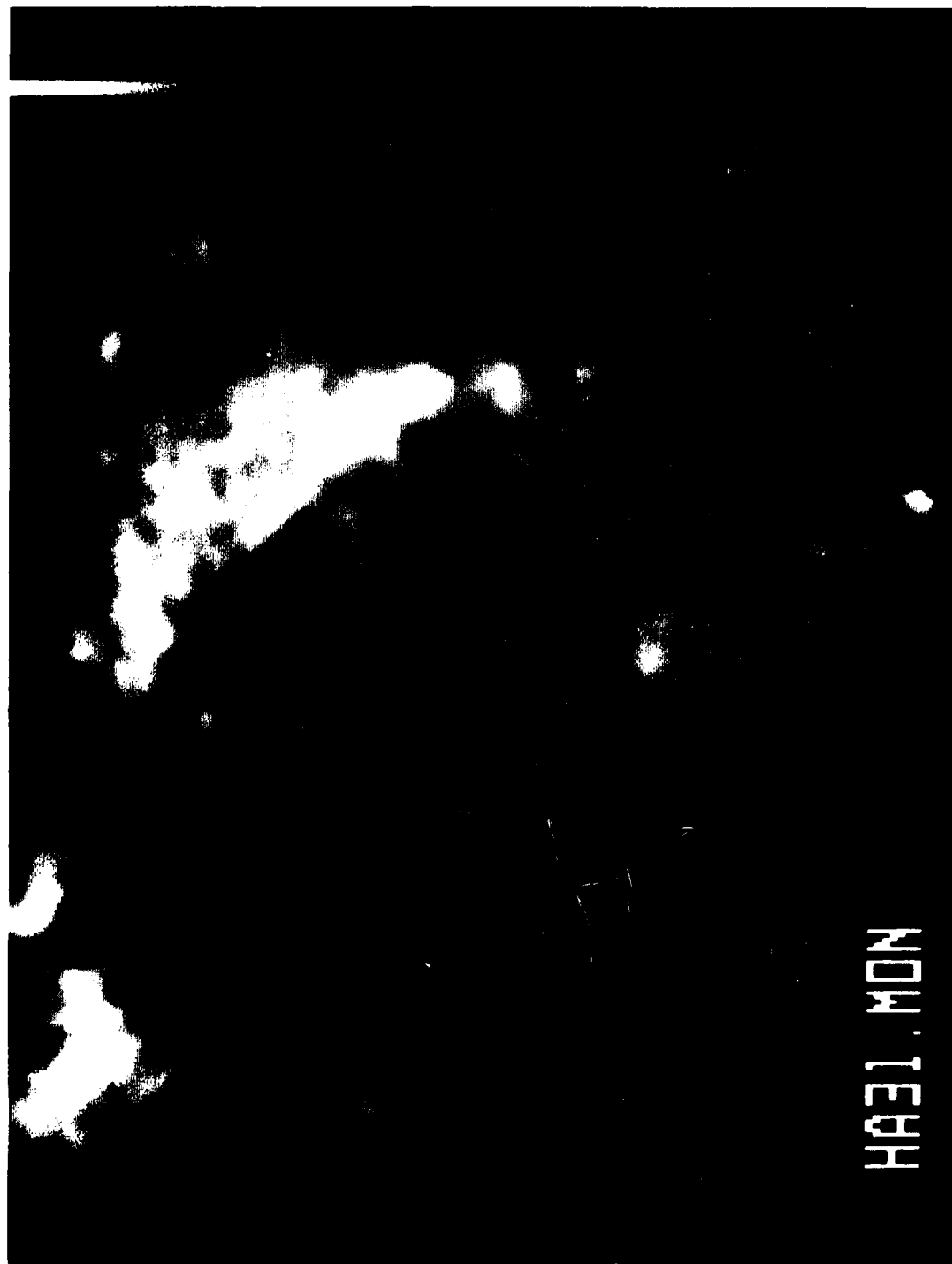
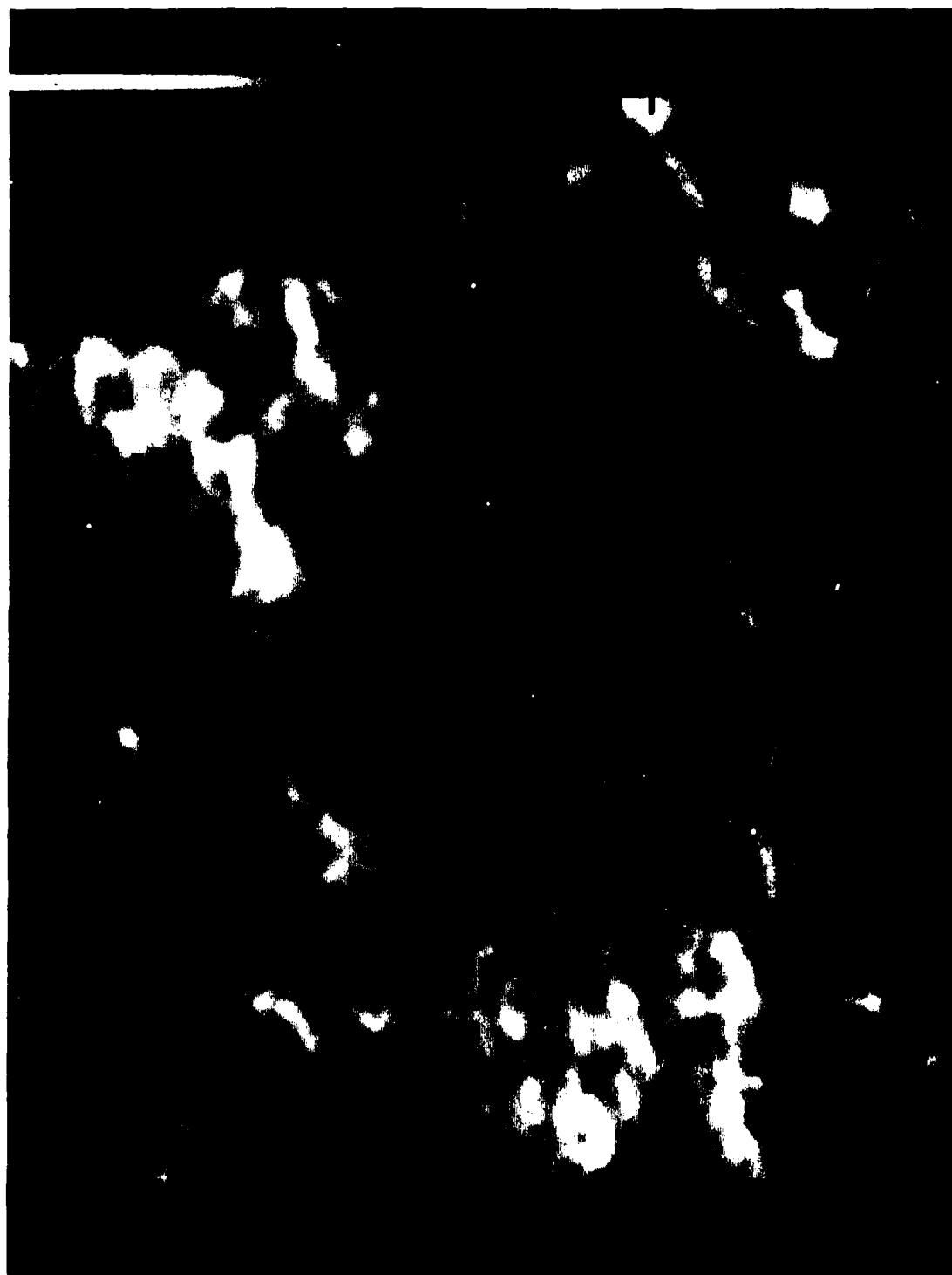


Image of the same region in the blue wing of H-alpha,  
at an offset of about 0.5 Angstroms, showing the low  
chromosphere.



**Image** of the same region in H-alpha line center, showing the chromosphere. Note the very bright plage in the vicinity of the newly erupting bipolar magnetic fields.



Magnetogram of a large cell on the edge of an active region, made in Mg I 5173 in very good seeing. Tick marks are 2 arcseconds. This represents the best seeing of the 1982 observing run; many flux tubes can be found at the pixel limit of resolution, 0.5 - 0.75 arcseconds.



Blue wing intensity in Mg I 5173 of the same region. A time series of 9 steps, spanning 25 minutes, exists but only the first and last step have been digitized. Seeing remains nearly this good throughout.

## APPENDIX B - ABSTRACTS

Abstract of Paper Presented at American Astronomical Society Meeting, Boston, January 1983.

Fine Structure in the Solar Magnetic Field,  
T. D. Tarbell, A. M. Title, Lockheed. We present observations made with the Spacelab 2 engineering model tunable filter at the Sac. Pk. Tower Telescope. The filter bandwidth is 75 mÅ at Fe I 5250, narrow enough to provide some line profile information. Images are recorded on film and analyzed digitally to make longitudinal magnetograms, Dopplergrams and photometrically-corrected filtergrams. The best frames have resolution better than 0.5 arcseconds. Results for several active regions are presented, illustrating the following: offsets between intensity and magnetic maps of faculae, predicted by magnetostatic flux tube models; variability in the relation between downdraft speed and magnetic flux; the spatial relationship between granulation and flux tubes of different sizes; greater inclination of field lines in dark penumbral filaments than in bright ones; extension of the penumbral fields far beyond the visible penumbral edge; a possible change in the magnetic fine structure of a complex active region during a flare. This work is supported by Lockheed IR funds and AFGL contracts.

Abstract of Paper Presented at the Fourth European Meeting on Solar Physics,  
"The Hydromagnetics of the Sun," Utrecht, October, 1984.

THE RELATIONSHIPS BETWEEN THE MAGNETIC FIELD  
AND THE CHROMOSPHERIC "BRIGHT POINTS"

L. DAME<sup>1</sup>, K. TOPKA<sup>2</sup>, A. TITLE<sup>2</sup>, T. TARBELL<sup>2</sup> and P. GOUTTEBROZE<sup>1</sup>.

(1) LPSP, BP 10, Verrières le Buisson 91371, FRANCE  
(2) LPARL, 3251 HANOVER St., PALO ALTO CA 94304, USA

Simultaneous high resolution observations of the magnetic field (Lockheed high resolution Tunable Lyot Filter) and 0.6 Å bandpass CaII K<sub>2v</sub> Filtergrams (Lockheed Birefringent Filter) were obtained in December 1983 at the Vacuum Tower Telescope of Sacramento Peak Observatory on a 2 by 2 arcmin area of active and quiet sun. The excellent quality and high resolutions both spatial (sub-arcsec) and temporal (12 sec exposure rate) on a 20 minute sequence allow a detailed comparison of the magnetic field occurrence and the chromospheric structures both in the network and in the supergranular cells where the magnetic field presence is compared to the CaII "Bright Points" locations. The influence of the chromospheric oscillatory field on the different structures and its implications on the correlation magnetic field - CaII intensities is also investigated.

Abstract of Paper Presented at American Astronomical Society Meeting, Tucson, January, 1985

A manuscript describing this work is being prepared for The Astrophysical Journal.

High Resolution Observations of Magnetic Features on the Sun

K.P. Topka and T.D. Tarbell (Lockheed)

The study of small, isolated, magnetic features on the sun reveals that they can apparently decay in place, without the simultaneous removal of an equal amount of observable opposite polarity flux. These results were obtained from a time sequence of 16 high resolution magnetograms (best have 1 arc sec resolution) covering 1 hour. The observations, made at Sac Peak Observatory, made use of the Lockheed Tunable Filter (engineering model for the Spacelab 2 SOUP experiment and an active optical system (sunspot tracker), during moments of good to excellent seeing. Differential geometric image distortion, due to atmospheric seeing, was removed using a cross-correlation technique. This allows for a more accurate point-by-point comparison of the magnetograms.

Twenty-eight small (2 to 8 arc sec diameters) magnetic features were selected for study on the basis that they were usually monopolar and well isolated from surrounding features. The total magnetic flux present was carefully measured for each feature on each magnetogram. About 1/3 of all of these features showed evidence for a decrease in the total amount of magnetic flux present during the 1 hour observing period, without any measurable simultaneous loss of an equal amount of nearby opposite polarity flux. In one case the decaying magnetic feature was very well isolated from any other feature, surrounded by a region with no detectable magnetic flux. During its decay, no detectable magnetic flux was observed to spread out into this surrounding region.

American Astronomical Society  
Abstract submitted for the 165th (Tucson) Meet

10-25-84

Date Submitted

FORM VERSION 8/84

Abstract of Paper Presented at American Astronomical Society Meeting, Tucson, January 1985.

A manuscript describing this work is being prepared for The Astrophysical Journal.

Magnetic Fields, Downdrafts, and Granulation in the Solar Photosphere

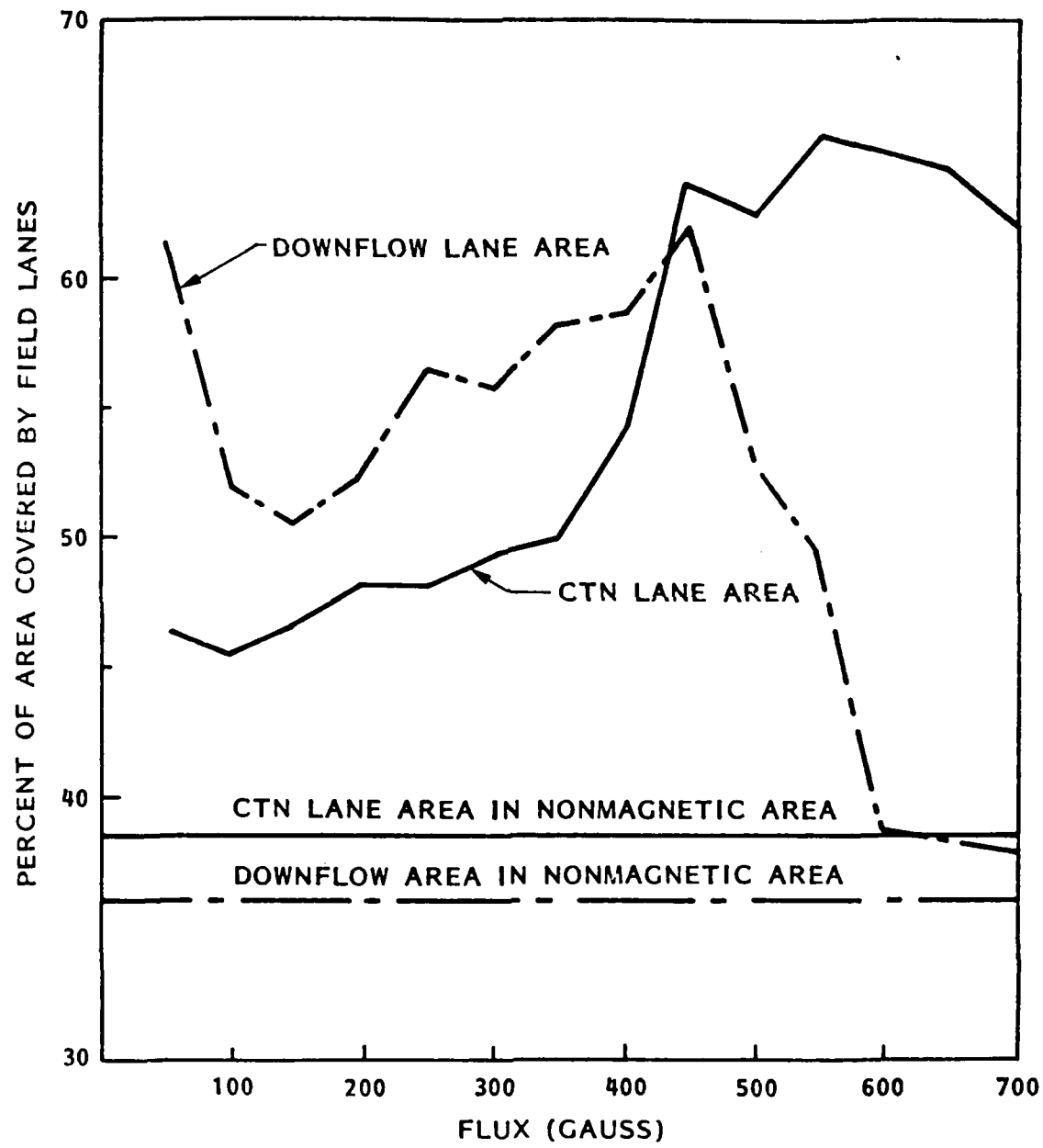
A.M. Title and T.D. Tarbell (Lockheed PARL)

We discuss very high resolution observations of quiet and active sun in the photospheric Fe I line 5250. These images were obtained on film at the Sacramento Peak Tower with a Lockheed tunable birefringent filter. When magnetograms and dopplergrams are coaligned and compared at this resolution (1/2 arc second), we find that the weaker magnetic flux concentrations are well correlated with downdrafts. This occurs for magnetogram signals in the 100 - 500 gauss range, presumably corresponding to area filling factors of 10 - 50 percent. These fields form a small scale network pattern, with "cell" diameters of 2 to 5 arcseconds; these are somewhat larger than the mean intergranular spacing of 2.4 arcseconds. Magnetic fields in this network correlate better with dark intergranular lanes than with bright granules in the coaligned continuum images. This relationship is less clear than the downflow correlation, because our observed granule-lane contrast is much less in magnetic than in non-magnetic photosphere (abnormal granulation). In stronger flux concentrations (500 - 1000 gauss), the downflow is suppressed compared with the weaker magnetic surround. These correspond to pores and "holes" in the continuum image. By holes, we mean transient spaces between the bright granules that are somewhat darker than average but not obvious pores. The time-scale for rearrangement of the small scale magnetic network is not currently known, but it is definitely longer than the 5 to 10 minute time-scale of granulation.

American Astronomical Society  
Abstract submitted for the 185th (Tucson) Meeting

Date Submitted 10-25-84

FORM VERSION 8/84



## APPENDIX C

Paper Presented at the NSO Conference, "Small-Scale Dynamical Processes in Quiet Stellar Atmospheres," Sunspot, NM, July, 1983.

### HIGH SPATIAL RESOLUTION MAGNETIC OBSERVATIONS OF AN ACTIVE REGION

Ken Topka and Ted Tarbell  
Lockheed Palo Alto Research Laboratory  
Dept 52-13, Bldg. 202  
3251 Hanover St  
Palo Alto, California 94304

#### ABSTRACT

High spatial resolution magnetograms of an active region reveal apparent changes in the magnetic flux of small isolated features on time scales less than 30 minutes. Both flux increases and decreases are observed, sometimes for a single feature. These changes are seen in small unipolar magnetic regions with no obvious changes observed in any nearby opposite polarity features.

#### 1. INTRODUCTION

The birth of an active region always results from the emergence of new magnetic flux from below the photosphere, never from the concentration of previously existing photospheric flux. Many new active regions are born each sunspot cycle, and this implies that a lot of new flux must emerge. An equal amount of flux must be removed from the photosphere each cycle as well, in order to prevent an ever increasing buildup of flux on the sun.

It has been known for some time that active regions decay on time scales of a few months. The flux appears to spread out by diffusion (cancelling where opposite polarities meet), until that which remains is indistinguishable from the background. More recently, significant flux changes in active regions on time scales of

a few days have been reported (Wallenhorst and Howard 1981) (Wallenhorst and Topka 1982). Wilson and Simon (1983) have reported flux changes in small magnetic regions on time scales of about 20 minutes.

The purpose of this paper is to report on the search for flux changes in small magnetic regions on time scales of a few minutes, similar to those reported by Wilson and Simon. The observations analyzed were selected on the basis of good time coverage and good seeing, rather than choosing a specific target or event.

## 2. OBSERVATIONS

The observations were obtained on 19 April 1980 (1427 UT - 1453 UT) of AR 2391, an older active region located at N 12, W 44. The equipment consisted of the Lockheed tunable filter (100 mA bandpass FWHM, engineering model for Spacelab 2 Solar Optical Universal Polarimeter; Title and Rosenberg 1981), mounted behind an image stabilization system that guides on a sunspot (Tarbell and Smithson 1981). The observations were carried out at the Sacramento Peak Observatory Vacuum Tower Telescope.

All images were recorded on photographic film. Fourteen images were recorded at each time step, six in the magnetically sensitive Fe I 6302.50 Å line (3 RCP + LCP pairs) and eight in H-alpha (wavelength scan from H-alpha + 2 Å to H-alpha - 2 Å). Magnetic pairs were taken in the blue wing of 6302, 60 mA from line center. The filter wavelength was calibrated periodically with a HeNe laser and found to be stable to within a few mA. The seeing was quite good and fairly uniform, permitting one-half to one arcsecond resolution despite the relatively long exposure times needed (0.5 seconds).

## 3. RESULTS

Fifty four images comprising 9 time steps (3 Fe I RCP + LCP pairs per time step) have been digitized (256 x 256 pixels) using the fast microphotometer at Sac Peak. Film densities are converted to intensities using a characteristic curve derived from exposure tests. One digital image at each time step was arbitrarily chosen as a standard. Each of the other five images at the same time step were subdivided into 16 equal parts, and each part was matched as closely as possible (via cross-correlation) to the corresponding part of the standard image. After this was performed for all 16 parts of each image, they were

stretched (bilinear interpolation between the measured offsets in X and Y) to correspond as closely as possible to the standard. This process does not remove all image distortion due to seeing, instead it stretches 5 of the images until they closely match the image distortion present in the sixth image at the same time step. The match is generally good to better than 1/4 to 1/2 pixel. Each RCP + LCP pair has been subtracted to produce 27 magnetograms. Point by point subtraction of a pair of images (1 RCP, 1 LCP) leads to the determination at each point of the V Stokes parameter ( $V = [RCP - LCP]$ ). For a uniform magnetic field parallel to the line of sight the magnetic field strength  $B$  is approximately proportional to  $V$ . More generally, the normalized magnetogram  $V/I$  (where  $I = RCP + LCP$ ) is approximately proportional to the magnetic flux averaged over the resolution element of the image. The 3 magnetograms at each time step were then averaged to produce 9 final magnetograms, one at each time step. The field of view is  $80 \times 80$  arc sec, and the limiting spatial resolution is about 1 arc sec.

Twenty two small, unipolar magnetic features were selected for study. Most features were isolated, to avoid apparent flux changes that are due to undetectable movement of magnetic features into and out of the region of study. Six were selected on the basis of visual inspection of the magnetograms (they appeared to change), and the rest were picked at random. A rectangular box was drawn around each feature, and the average Stokes  $V/I$  was determined in each box for all 9 magnetogram frames. The average Stokes  $V/I$  was multiplied by the area of each box to yield the net magnetic flux present (in arbitrary units, since all we are interested in here are flux changes. Later we discuss estimates of the actual amount of magnetic flux involved). The boxes ranged in area from 4 to 40 square arc sec, depending upon the size of the magnetic feature enclosed. The boxes were made large enough so that slight shifts of a magnetic feature (from one magnetic frame to the next) due to image distortion induced by atmosphere seeing does not seriously affect the results.

There were significant fluctuations in the zero points of the magnetograms from one frame to the next, due in part to slight changes in density with position on each original photographic frame. A local background (a field free area that is as close as practical to each feature) was chosen. Subtraction of the local background significantly reduced frame to frame fluctuations, and the typical small feature showed a maximum variation of about 10% in the measured flux values, with no trends discernable. Four small magnetic regions with no flux changes greater than the fluctuations described above are shown in figure 1.

Other features, however, showed systematic changes in the measured magnetic flux that were much greater than the 10% maximum found for most small magnetic regions. One feature, for example, lost almost 90% of its flux in about 10 minutes. Figure 2 shows 5 examples of features with apparent changes in flux. Included in figure 2 are flux decreases, increases, and both increases and decreases for a single feature (flux decay followed by recovery). In one case the possible movement of flux from outside to inside of the box containing a feature may explain some of the observed flux change. Feature 5 appeared to decay while new flux emerged nearby. Some of this new flux appears to have migrated into the area near feature 5, thus causing an apparent recovery of flux (see figure 2). The box containing feature 5 was only about 4 square arc seconds in area, and it was not possible to shift it around to completely avoid the new emergence without excluding part of feature 5. No evidence for flux migration was seen for the other features. The 5 features of figure 2 had the most pronounced trends of the 22 studied, and all were selected because they appeared to be changing visually. Most of the rest of the features studied had no discernable trends in their measured magnetic fluxes, similar to the 4 features shown in figure 1. Less than 5% of the total magnetic flux present within our magnetogram field of view is contained in these 22 features.

Table 1 lists estimates of the amount of magnetic flux initially present in each of the features shown in figure 2, as well as the change in flux, the time for this change to occur, and the rate of change of flux. The magnetogram signals (V/I) have been converted to magnetic flux using the slope of the 6302 line profile in similar magnetic elements, measured from wavelength scans with the same filter. While this calibration could be wrong by as much as 50%, we are concerned here with the temporal changes, not with the absolute values. From the line profile scans, we can infer that changes in Doppler shifts of several km/sec would be needed to affect the flux measurements at the levels observed.

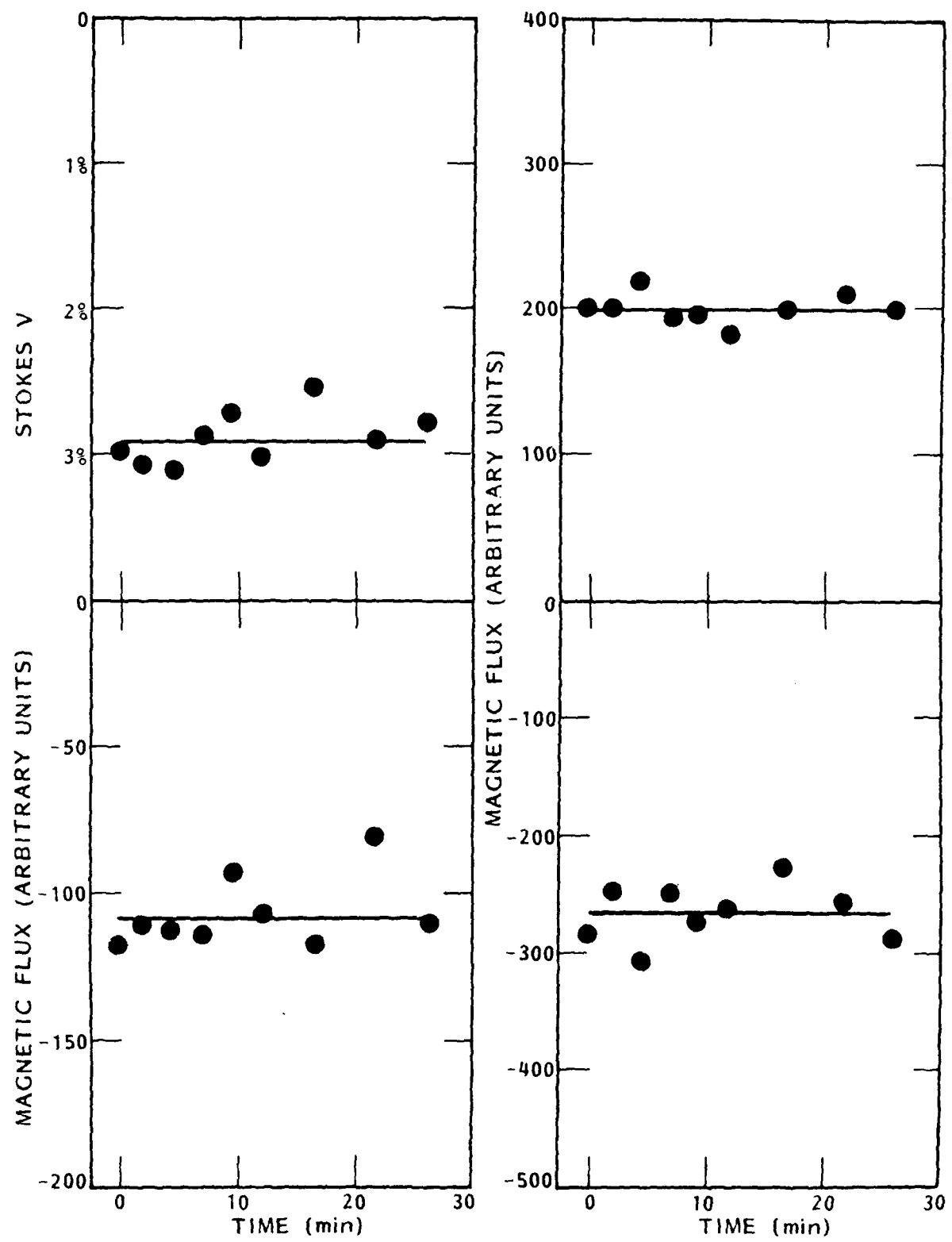


Figure 1. The magnetic flux (or Stokes parameter V for the upper left plot) is shown as a function of time for 4 different isolated features. The straight lines through the data points represent the average value. No strong flux increases or decreases are apparent in these data.

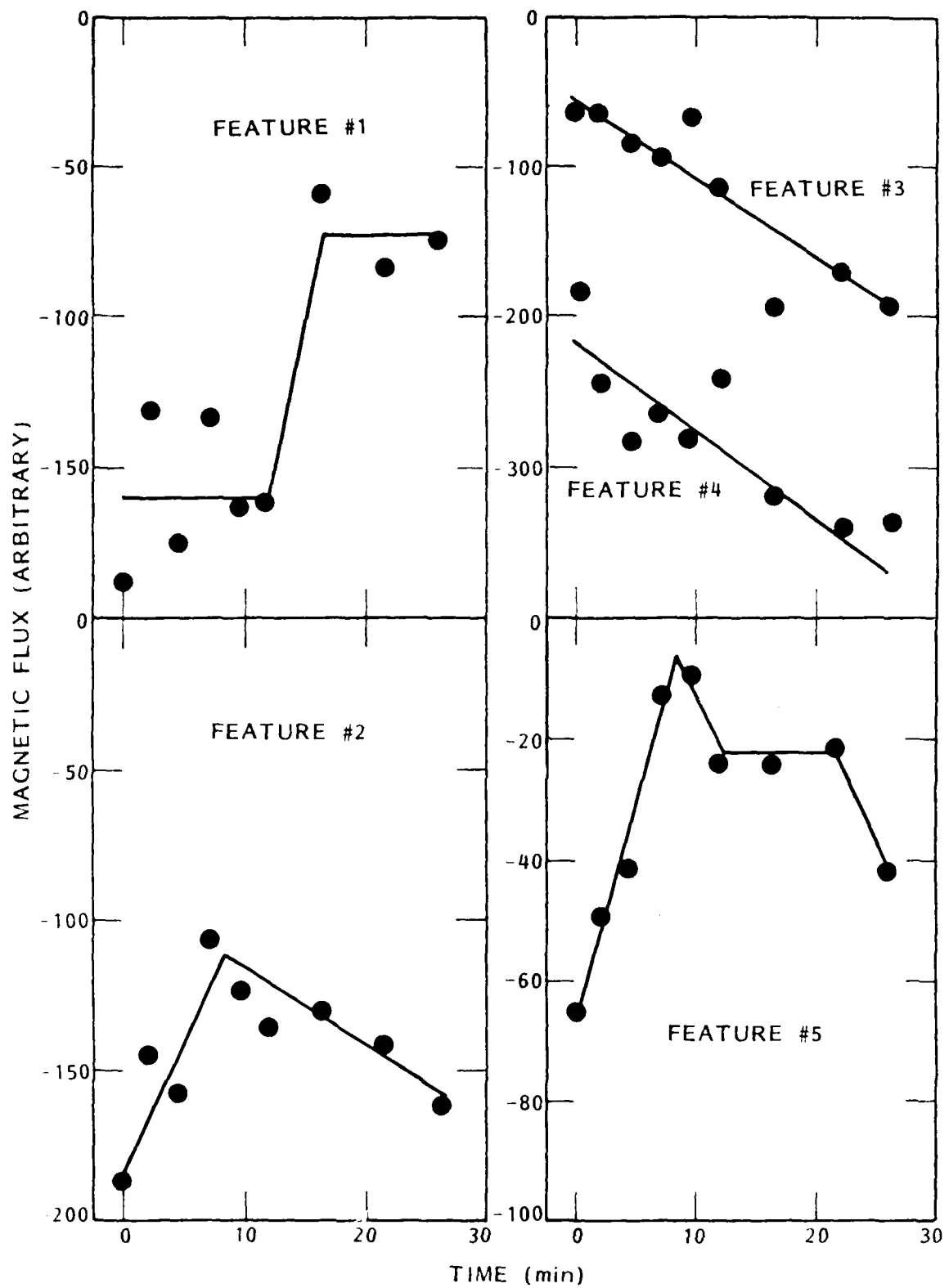


Figure 2. The magnetic flux for 5 different isolated features is shown plotted as a function of time. Both flux increases and decreases as apparent, as indicated by the trend lines.

TABLE 1. MEASURED FLUX CHANGES IN SMALL MAGNETIC REGIONS

FEATURE	INITIAL FLUX ( $\times 1.0E+18$ Mx)	CHANGE IN FLUX ( $\times 1.0E+18$ Mx)	TIME (min)	RATE OF CHANGE ( $1.0E+15$ Mx/s)
1	9.4	-5.4	4.7	-19
2	10.2	-3.7	7.2	-8.6
2	6.5	+2.7	18.8	+2.4
3	3.5	+7.7	26.0	+4.9
4	10.0	+9.2	26.0	+5.9
5	3.8	-3.3	9.5	-5.7

Note: The initial flux given in column 2 is absolute value. The - sign in column 3 denotes flux decreases, + sign flux increases.

#### 4. DISCUSSION

Because the divergence of the magnetic field vector  $B$  is zero, an eruption of positive magnetic polarity flux must be accompanied by a simultaneous and equal eruption of negative polarity flux. The typical picture for this process is the emergence through the photosphere of a loop consisting of one or more 'flux tubes', due to the magnetic buoyancy of the loop and/or convective upflows. As the loop emerges two footpoints of opposite polarity form that move apart (Zwaan 1978). This process has been observed in similar filter data of other active regions.

The long term decay of an active region is probably due to diffusion. Since magnetic field lines are 'frozen' into the photospheric and subphotospheric material, they will be carried along with any flows in this material. The magnetic field lines are assumed to random-walk away from their points of emergence, and magnetic features may further spread out due to Ohmic dissipation. When opposite polarities eventually meet they 'cancel', a process that results in the net removal of flux from the photosphere.

However, there now exist observations that suggest that processes other than those described above are present on

the sun. The process of emergence has been observed where only one polarity flux is observable, thus contradicting the view the two footpoints of equal and opposite polarity that move apart must always be seen. In some cases no observable increase in the flux of the opposite polarity is seen anywhere near the site of the emergence (and in fact, in some cases no opposite polarity flux is detectable at the site of the emergence at all). The observations of Wilson and Simon (1983) include this phenomenon, as do the observations reported in this paper. We do not suggest that magnetic monopoles exist on the surface of the sun. The missing polarity flux is there, somewhere, and may be undetectable in our magnetograms for some reason. In any case, the phenomenon is not yet understood.

The decay of an active region via diffusion requires long time scales (months) for the removal of significant amounts of photospheric flux. Recent observations show possible flux removal from active regions on much shorter time scales than is expected from diffusion, again suggesting other mechanisms exist. Howard and La Bonte (1981) made the rather startling claim that fully 10% of the magnetic flux present on the sun today was not there yesterday, implying that emergence and disappearance of flux to and from the photosphere is nearly continuous, and that large amounts can be added or subtracted on relatively short time scales. Wallenhorst and Howard (1982) and Wallenhorst and Topka (1982) observed that a substantial fraction of the entire flux of an active region can apparently be removed from the photosphere in just a few days. The observed decay rates were up to 10% of the total flux of the active region per day. Furthermore, Wallenhorst and Topka (1982) obtained higher resolution magnetograms (best were 2 arc sec, typical was 2-3 arc sec). These magnetograms seemed to show a general weakening of the active region, even in large unipolar areas far removed from the neutral line. Magnetic flux was just fading away in place, rather than coming together with equal and opposite polarity flux at the neutral line and disappearing there.

Wilson and Simon (1983) reported flux decreases on very short time scales (less than 1 hour), without any observable changes in nearby opposite polarity flux. In these observations the entire line profile (6302 Å) was used, instead of just a narrow band pass in the wings of the line (as in a conventional Babcock magnetograph). It is hard to see how instrumental effects or line profile effects could have caused the flux changes. Although the observations reported here are of the magnetograph type that uses only the blue wing of the line, they show essentially the same sorts of flux increase and decay. The phenomena of emergence and of 'disappearance in place' of one polarity of flux, without any observable opposite polarity flux emerging

or disappearing nearby, has potentially interesting theoretical consequences if confirmed.

### 5. ACKNOWLEDGEMENTS

We want to thank the Tower staff and our Lockheed colleagues Harry Ramsey, Ron Sharbaugh, and Bob Smithson for obtaining the observations analyzed here. We also thank Alan Title and Aad Van Ballegooijen of Lockheed and Peter Wilson of the University of Sydney for useful comments and discussions. Larry November of Sac Peak provided essential help with the microphotometer, and Stuart Ferguson and Chris Rhode assisted in computer programming at Lockheed. This work was supported by AFGL contracts and Lockheed Independent Research Funds.

### REFERENCES

- Howard, R., and LaBonte, B. 1981, *Solar Phys.* 74, 131.
- Tarbell, T., and Smithson, R. 1981, in *Solar Instrumentation: What's Next*, ed. R.B. Dunn, (Proc. Sacramento Peak National Obs. Conference), 491.
- Title A., and Rosenberg, W. ibid, 326.
- Wallenhorst, S.G. and Howard, R. 1982, *Solar Phys.*, 76, 203.
- Wallenhorst, S.G. and Topka, K.P. 1982, *Solar Phys.*, 81, 33.
- Wilson, P.R., and Simon, G.W. 1983, *Astrophys. Jour.*, in press.
- Zwaan, C. 1978, *Solar Phys.*, 60, 213.

APPENDIX D

Manuscript Submitted to the Astrophysical Journal.

THE DISAPPEARANCE OF MAGNETIC FLUX IN SOLAR ACTIVE REGIONS

A.A. van Ballegooijen and A.M. Title

Lockheed Palo Alto Research Laboratory

Palo Alto, California

and

H.C. Spruit

Max Planck Institut fur Physik und Astrophysik

Garching bei Munchen, F.R.G.

Proposed for: Astrophysical Journal

## ABSTRACT

We present a critical analysis of observations of the decay of large active regions, and we propose that magnetic flux disappears more rapidly than can be explained with Leighton's diffusion model. The proposed component of the flux disappearance seems to take place locally, without any apparent motion of magnetic elements, and does not seem to involve the submergence of magnetic flux.

To explain these observations we propose a model, in which part of the observed large-scale field of active regions is annihilated by small-scale fields that emerge in between patches of opposite polarity. The small-scale field is assumed to consist of a train of dipoles, each with typical size of 1000 km and flux of  $10^{17}$  Mx, and with an orientation opposite to that of the active regions as a whole. The interaction of these dipoles with the overlying coronal field leads to the decay of the active region, without any apparent large-scale motion of magnetic features in the photosphere.

To show that such a scenario is not physically unreasonable, we describe a possible mechanism by which the small-scale field might be formed. According to this model, part of the active-region field reconnects deep below the solar surface, leading to the formation of U-shaped magnetic loops in the convective zone. During the decay of the active region, these U-loops float to the surface, where they emerge as trains of small dipoles. Due to the large amount of mass captured in the U-loop, the predicted field strength of the dipoles is only a few Gauss.

Subject Headings: hydromagnetics -- sun: activity

sun: -- magnetic fields

## 1. INTRODUCTION

Magnetic flux first appears at the solar surface in the form of easily identified, bipolar active regions. The emergence of flux in both large and small active regions takes place in a similar way, and is fairly well understood observationally: a loop of magnetic field breaks through the solar surface from below, and the opposite polarity footpoints of the loop, as seen in photospheric magnetograms, separate as the loop rises up through the atmosphere (Bumba and Howard 1965; Zwaan 1978; Sheeley 1981). Presumably, the flux of active regions originates from a horizontal field located at some level in the convective zone. Large active regions, with flux greater than  $10^{21}$  Mx, probably originate from the deep layers of the convective zone (e.g. Parker 1975, 1984a; Golub et al. 1981).

In comparison with flux emergence, the disappearance of magnetic flux from the surface is much less well understood (Zwaan 1978). As the field of an active region is dispersed across the solar surface, the measured flux is seen to decrease, and ultimately the region disappears into the background field. It has been presumed that most of the flux disappearance takes place in regions where opposite polarity fields meet at neutral lines, and in areas of mixed polarity. The fact that flux-disappearance is not a dramatic process indicates that it probably occurs on small length-scales, and involves only small amounts of flux at a time. Leighton (1964) proposed that the intermixing of opposite polarity fields, due to random motions induced by supergranulation, plays an important role during the late phases of

evolution of active regions. In Leighton's model the action of the supergranular motions on the field is described as diffusion, which implies a certain relation between dispersal and decay of the field.

However, it has been suggested, e.g. by Wallenhorst and Topka (1982), that another process of flux-disappearance takes place as well. The observations of Wallenhorst and Topka suggested that part of the active-region flux disappears locally, without any apparent motion of field towards the neutral line; the two patches of opposite polarity just fade away. This seems in contradiction with our theoretical understanding: due to the high conductivity of the solar plasma, the field is expected to be "frozen" into the gas, so that the evolution of the magnetic field is due primarily to the motions of the plasma; magnetic diffusion is thought to play an insignificant role. Then it seems that the only way in which flux can be annihilated is when elements of opposite polarity move towards each other until they merge and disappear. Since the opposite polarities in a large active region typically are 50,000 km away from the neutral line, we would expect to see motions of magnetic features over at least this distance during the decay of the region. The observed decay of the flux without any significant spreading or dispersal of the field thus poses a difficult theoretical problem, which we will address in the present paper.

The paper is set up as follows. In Sect. 2 we discuss various observations of active-region decay, with the purpose to extract further evidence for the proposition that part of the flux disappears locally. In an attempt to explain these observations we propose, in Sect. 3, a qualitative model of the decay of a large active region, in

particular regarding the dynamics of the sub-surface magnetic field. We consider an isolated active region, i.e., we neglect possible interactions with other active regions, ephemeral regions, or other background fields.

## 2. OBSERVATIONS OF FLUX DISAPPEARANCE

In the following we discuss various observations related to the disappearance of flux, in order to identify the mechanisms by which this process takes place.

### a) Large-scale characteristics

In the course of the solar cycle a large number of active regions appear, yet there is no large build-up of field at the surface. This implies that most magnetic flux disappears on a short timescale. The average lifetime of magnetic flux at the surface may be estimated in a number of ways. One method is to divide the total amount of flux present on the surface at any one time by the rate of emergence of large active regions. Observations by J.W. Harvey (1983, private communication) indicate that on average about  $4 \cdot 10^{23}$  Mx of each polarity was present on the solar surface during the maximum of cycle 21. (This flux-value has not been corrected for the effects of line-profile changes in sunspots, nor for the fact that, at high latitudes, only the line-of-sight component of the field was observed; however, these corrections are probably small). The rate of flux emergence during the Skylab period in 1973 was discussed by Golub et al. (1976, 1979). They estimated that active regions with lifetimes of a few days or more contributed about  $8 \cdot 10^{21}$  Mx/day. For the year 1956, Sheeley (1981) estimated an emergence rate of  $3 \cdot 10^{21}$  Mx/day for regions with lifetimes of at least 10 days. These observations

suggest that an emergence rate between about  $3 \cdot 10^{21}$  and  $10^{22}$  Mx/day is typical for solar maximum. Combining this with Harvey's value for the surface flux, we find that the average lifetime of the flux in large active regions is between 1 and 4 months.

A somewhat different method to estimate the lifetime is that of Howard and LaBonte (1981), who measured flux changes in regions  $13.2^{\circ}$  in longitude and  $3.4^{\circ}/\cos\lambda$  in latitude over a period of 3 days near central meridian passage. They found that flux appears and disappears at a rate that is sufficient to replace all existing flux in about 10 days, from which we infer that the flux typically changed by 30% over the 3-day observing period. Positive and negative flux changes occur in equal numbers, and with the same amplitude. Although this 10-day timescale is significantly shorter than that estimated from the emergence-rate of active regions, it should be kept in mind that the method of Howard and LaBonte (1981) provides only a lower limit to the average lifetime. Since it is not known how long a period of flux increase or decrease lasts, it is possible that a 10% flux decrease per day persists only for about 3 days, and is followed by a flux increase. Then the net effect is a much slower change, with a time constant longer than 10 days.

Rapid disappearance of flux is also suggested by the observations of Gaizauskas et al. (1983), who looked for large-scale patterns in the emergence of solar active regions. Using synoptic maps of the magnetic field over 27 solar rotations obtained from Kitt Peak magnetograms, they identified complexes of activity. These are series of apparently related active regions that emerge near the same longitude and latitude over a period of 3 to 6 rotations. An

important aspect of these activity complexes is that they are maintained by fresh injections of magnetic flux in the form of distinct bipolar regions, while the flux of earlier regions disappears. In the case of one particularly large complex it was shown that the magnetic flux remained nearly constant at  $7 \cdot 10^{22}$  Mx during 6 rotations, even though large new regions kept appearing at an average rate of one every 7 days. As Gaizauskas et al. (1983) point out, this indicates that flux disappearance in this complex takes place *in situ*, i.e., the flux is not dispersed across the solar surface. When a complex dies the flux disappears on a timescale of only one or two months. This also seems consistent with the observations of J.W. Harvey (1983, private communication), who found that the total flux of the sun fluctuates by about 20%, or  $7 \cdot 10^{22}$  Mx, over a period of 2 solar rotations; these variations may well be due to the birth and decay of activity complexes.

### b) Diffusion models

The spreading of active region magnetic fields across the solar surface has been studied by a number of authors. Leighton (1964) showed that the dispersal of unipolar and bipolar magnetic regions can be described fairly well as a diffusion process, i.e., the flux  $n(r,t)$  per unit area satisfies the diffusion equation:

$$\frac{\partial n}{\partial t} = D \nabla^2 n, \quad (1)$$

where  $D$  is the diffusion constant, and  $\nabla^2$  is the Laplacian operator on the surface of a sphere. Leighton ascribed the diffusive action to

supergranulation, which moves the magnetic elements about in a random-walk fashion. The interdiffusion of opposite polarity field brings elements of positive and negative flux close together and leads to the disappearance of these elements. The rate at which opposite polarity fields interdiffuse depends on the magnitude of the diffusion constant. The value of the diffusion coefficient  $D$  used by Leighton was between 780 and 1550  $\text{km}^2/\text{s}$ .

A more refined estimate of the diffusion constant was given by Mosher (1977), who used several independent methods to determine  $D$ . From the rate of separation of opposite polarities in long-lived active regions Mosher estimated that  $D \approx 200 \text{ km}^2/\text{s}$ ; this estimate takes into account the effect of differential rotation on the evolution of the flux distribution (Leighton, 1964). Observations of the rate of area increase of magnetic regions are consistent with this estimate. The observed lifetimes of active regions yield  $D = 260 - 770 \text{ km}^2/\text{s}$ , depending on the assumed value of the threshold fieldstrength below which weak fields become undetectable. Mosher (1977) also measured the diffusion coefficient from the observed motion of magnetic features over short periods of time (hours to days). Using different data sets and methods of analysis, values of  $D$  between 140 and 300  $\text{km}^2/\text{s}$  were found. Mosher concluded that, within a factor 2, the diffusion constant  $D = 200 \text{ km}^2/\text{s}$ , and that the spreading of magnetic field over periods of months can indeed be represented as a diffusion process.

However, Mosher (1977) points out that the decay of the active region flux seems to be more rapid than can be explained with intermixing due to diffusion with  $D = 200 \text{ km}^2/\text{s}$ . To illustrate his

concern, Mosher considered a simple model of an active region, in which all positive flux is initially located at a point  $x = +a$ , and all negative flux at  $x = -a$ , on the  $x$ -axis;  $N_0$  is the initial source strength in Maxwells. The dispersal and intermixing of flux as function of time  $t$  is described by Eq.(1), which yields the solution:

$$n(x, y, t) = \frac{N_0}{2\pi Dt} \exp\left(-\frac{x^2+y^2+a^2}{4Dt}\right) \sinh\left(\frac{xa}{2Dt}\right). \quad (2)$$

Here  $x$  and  $y$  are horizontal coordinates, and effects due to the curvature of the solar surface have been neglected. The net surviving flux (of one sign) at time  $t$  is obtained by integrating  $n(x, y, t)$  over the half-plane  $x > 0$ :

$$N_+(t) = N_0 \operatorname{erf}\left(\frac{a}{\sqrt{4Dt}}\right), \quad (3)$$

where erf is the error function (see Abramowitz and Stegun 1965). According to this model approximately half the initial flux has disappeared at time  $t = t_0 = a^2/D$ . However, the remaining flux disappears rather slowly, since  $N_+ \approx 0.56 N_0 (t_0/t)^{1/2}$  for  $t \gg t_0$ ; for the flux to drop below 20% of its initial value we must wait until  $t = 7.8 t_0$ . For an initial separation of  $2a = 6 \cdot 10^4$  km and a diffusion constant  $D = 200 \text{ km}^2/\text{s}$ , the timescale  $t_0 = 52$  days, so that 20% of the flux still remains after 13 months. But in reality very little flux remains, even of large active regions, after only 6 months.

This enhanced decay rate explains why the diffusion constant, deduced by Mosher (1977) from the observed lifetimes of active regions, was somewhat larger than  $200 \text{ km}^2/\text{s}$ : to reproduce the actual flux-decay rate with a diffusion model, a larger diffusion constant is

necessary. Mosher suggested, however, that no great significance should be attached to these facts, since his flux estimates were obtained by visual inspection of magnetograms with a lowest contour level of 5 Gauss, and consequently his flux measurements are rather crude. He also proposed the existence of a poleward meridional flow that transports the weak remnant fields out to higher latitudes. This meridional flow sweeps clean the low-latitude active belts, thus preventing the build-up of magnetic fields there.

Although the presence of a meridional flow has been reported by other observers (Beckers 1979; Howard 1979; Duvall 1979; LaBonte and Howard 1982; Topka et al. 1982), we suggest that meridional motions alone are not sufficient to explain the rapid decay of active regions. Also, we believe that the difference between the observed flux and the flux predicted by the diffusion model (with  $D = 200 \text{ km}^2/\text{s}$ ) is too large to be due to observational uncertainties. In our opinion the lack of a long-term residue of active regions points to a more fundamental problem with the diffusion model.

Recently, Sheeley et al. (1983), Boris et al. (1983), and Sheeley et al. (1984, in preparation) have studied the decay of a number of isolated active regions, using Kitt Peak magnetograms. They determined the value of the diffusion constant  $D$  by comparing two magnetograms, taken one or more rotations apart, with the results of a diffusion model. This model includes the effects of differential rotation and meridional flow on the flux distribution. In contrast with Mosher's study, the method is sensitive both to the shape of the magnetic contours and the amount of flux in the region. In 15 out of 18 cases the authors find values of  $D$  between 280 and  $600 \text{ km}^2/\text{s}$ , with

an average of  $430 \text{ km}^2/\text{s}$ , somewhat higher than the value found by Mosher (1977). The remaining three cases have  $D \geq 970 \text{ km}^2/\text{s}$ , the cause of which is unknown.

We suggest that the difference between the  $430 \text{ km}^2/\text{s}$  of Sheeley et al. (1984), and the  $200 \text{ km}^2/\text{s}$  of Mosher (1977), is real and is due to the fact that Mosher did not try to fit the observed flux. Although the dispersal of magnetic fields on the surface is well represented by diffusion with  $D = 200 \text{ km}^2/\text{s}$ , the rate of flux disappearance is too large to be explained in this way. We suggest that a significant fraction of the flux disappears locally, i.e., without the intermixing of opposite polarity fields. Fitting the magnetograph data with a diffusion model, Sheeley et al. have determined an effective "diffusion" constant ( $D_{\text{eff}} = 430 \text{ km}^2/\text{s}$ ) that includes the effects of enhanced flux decay.

Marsh (1978) has suggested that ephemeral active regions (cf. Martin and Harvey 1979) may cause an enhancement of the diffusion constant. Interactions between ephemeral regions and network elements in the quiet sun have recently been observed by Martin (1983). Reconnection of one of the poles of an ephemeral region with a neighboring network element is equivalent to the displacement of this element over a distance on the order of the pole separation of the region. Marsh (1978) estimated that the effective diffusion constant due to this process is about  $800 \text{ km}^2/\text{s}$ . We suggest, however, that ephemeral regions are important only for the diffusion of weak fields, i.e., during the late decay-phase of an active region, and in the "quiet" sun outside active regions. The reason is that, in strong magnetic fields, ephemeral regions do not have sufficient flux to

affect the network elements. Marsh (1978) made two assumptions, which restrict his analysis to a particular fieldstrength: (1) it was assumed that ephemeral regions fully reconnect with network elements, so that each pole of the ephemeral region must have the same flux as a network element; (2) the number density of network elements was taken to be independent of the average fieldstrength ( $2 \cdot 10^{-9} \text{ km}^{-2}$ ). Since each pole of a typical ephemeral region has about  $1.5 \cdot 10^{19} \text{ Mx}$  (Golub et al. 1977), Marsh's estimate of  $D$  applies only if the average fieldstrength in the network is about 3 Gauss. In fact the process can no longer be described as a diffusion process, since the "effective diffusion constant" depends on the average fieldstrength of the "diffused" flux. It is not clear how Eq.(1) should be modified to include the effects of ephemeral regions. However, the ephemeral-region effects are not important for the rapid decay of large active regions, since the fieldstrengths are larger than 3 Gauss in this case.

### c) Small-scale characteristics

Observations of the merging and disappearance of opposite polarity fields in a relatively quiet region on the sun have recently been described by Martin (1983). In the quiet sun, network elements, and poles of bipolar ephemeral regions, are seen to move about more or less randomly. Occasionally, opposite polarity elements collide, and the flux in each element is seen to decrease, until the smaller element completely disappears. The question arises whether the same process could be responsible for the disappearance of flux in large

active regions, i.e., does the flux in active regions disappear due to the random coalescence of small-scale, opposite polarity fields?

Wallenhorst and Howard (1982) studied changes in magnetic flux around the time of sunspot disappearance. Since the flux was measured using a magnetograph which saturates at a fieldstrength of about 300 Gauss, the sunspot fields are severely underestimated. Therefore one should expect to see an increase in the apparent flux of the active region as the sunspot initially dissolves. However, the opposite was found: there is a decrease of flux at or near the time the sunspot vanishes. This indicates that the flux lost by the sunspot disappears from the solar surface on a timescale of only 1 or 2 days.

Wallenhorst and Topka (1982) pointed out that the disappearance of flux does not seem to take place at the neutral line of the active region. Rather, the magnetic features that move away from the dissolving sunspot travel to the surrounding network across a relatively field-free "moat" (cf. Sheeley 1969; Harvey and Harvey 1973). When they reach the outer boundary of the moat the motion stops and the flux elements seem to gradually fade away in place. There is no evidence for motion of these features toward the neutral line of the region, which is far removed from the part of the moat boundary where the flux elements disappear. The flux released in the break-up of the spot apparently does not end up in the surrounding network.

These observations suggest that the disappearance of flux in large active regions is not due to the random intermixing of opposite polarity fields: flux disappears before intermixing can take place,

consistent with our analysis of the diffusion model (see above). In the next section a possible explanation of this phenomenon will be discussed.

#### d) Summary

We suggest that there are two different processes by which flux disappearance takes place. One process occurs over long periods of time, and is relevant to the later stages of dispersal and decay of large active regions. It is caused by the intermixing of opposite polarity fields induced by supergranulation and granulation. On length-scales large compared with the size of supergranules, this process can be reasonably well described as diffusion (Leighton 1964). On small length-scale the flux disappears by submergence. For average fieldstrengths less than a few Gauss, ephemeral regions may cause an enhancement of the diffusion rate.

However, another process of flux disappearance seems to take place as well. In large active regions, part of the flux is removed by a process that seems to involve the annihilation of fields at a distance: bodily motion of magnetic features towards the neutral line is not observed, and flux seems to disappear "in place" (Wallenhorst and Topka 1982). As a result of this process, active regions decay more rapidly than can be explained with diffusion models.

### 3. FLUX DISAPPEARANCE

#### a) Submergence

It has been suggested (e.g. Zwaan 1978; Parker 1984a; van Ballegooijen 1982) that flux disappearance can occur by submergence of magnetic field. When two flux tubes of opposite polarity move closer together in the photosphere, the field above the surface may reconnect, and form a flux loop. As sketched in Figure 1, this loop may be pulled down below the surface by the tension in the magnetic field. Tension forces can overcome the buoyancy forces only if the curvature at the top of the loop is sufficiently large. Presumably, convective flows below the surface play an important role in bringing the flux elements closer together, thereby increasing the loop curvature.

As seen with a high-resolution vector magnetograph, the process of submergence would look as follows. Two patches of opposite polarity field would be seen to come closer together, until they finally merge and disappear. Just before the moment of disappearance the magnetic field would be seen to turn horizontal. We suggest that the disappearance of magnetic elements in the quiet sun, observed by Martin (1983), may indeed be due to reconnection and submergence. The flux-decrease observed by Martin begins when the separation of the magnetic features is on the order of the spatial resolution (about 3000 km). We suggest, however, that the actual submergence process takes place on an unresolved scale. The submergence of a magnetic loop through the photosphere requires that the magnetic curvature

force at the top of the loop,  $B^2/(4\pi R)$ , be larger than the buoyancy force,  $B^2/(8\pi H)$ , i.e., the curvature radius  $R$  must be smaller than twice the photospheric scaleheight  $H$ . Since the separation of the footpoints at the base of the photosphere is about  $2 R$ , the flux elements must approach each other to within a distance of  $4 H$ , or about 500 km, before submergence can take place. Thus, the observed flux-decrease at 3000 km separation must be an effect of the spatial resolution of the instrument, since at this time the buoyancy is still too large to pull the flux loop down through the photosphere. The loop must also be fragmented before it can disappear: because of the minimum separation of 500 km, the thickness of each fragment can be a few hundred kilometers at most. Therefore we suggest that only small amounts of flux, of order  $10^{18}$  Mx or less, are involved in each event (assuming an actual fieldstrength of 1000 Gauss in the photosphere).

b) Emergence of reverse-polarity fields

One aspect of the submergence model is that flux elements have to move towards each other for flux disappearance to take place; the process can occur only near neutral lines, and in regions of mixed polarity. However, the observations discussed in Sect. 2 seem to indicate that during the decay-phase of active regions part of the magnetic flux disappears locally, without any motion of the field towards neutral lines. To explain these observations we propose that a different process of flux disappearance takes place as well. This process, sketched in Figure 2, involves the emergence of a train of small, reverse-polarity dipoles in between the two patches of opposite

polarity of the active region. The separation of elements in each dipole increases with time, bringing opposite-polarity elements of neighboring dipoles closer together. The magnetic field above the surface then adjusts itself by opening up the old dipoles, and forming new dipoles that connect the approaching elements. The first and last dipole in the train are forced to reconnect with the original patches of field. Subsequently, the newly formed dipoles disappear by submergence; in the process a fraction of the original field also disappears. It is important to note that, in the process described above, there is no motion of opposite polarity elements over large distances across the solar surface. The combined effect of the motions within all the dipoles (emergence, reconnection and submergence) is the same as the transport of flux over a large distance, but a single magnetic element does not travel over this large distance. As a result, flux seems to disappear in place.

The emergence of reverse-polarity dipoles in decaying active regions has not been observed. Thus, if the process indeed occurs, it must take place on a length-scale at or below the spatial resolution of the instruments; the sensitivity of the magnetographs also plays a role. These observational constraints limit the possible size of the dipoles to about 1000 km, and the maximum allowable fieldstrength on this scale is about 10 gauss. The following calculation shows, however, that a sufficient amount of flux could emerge in such dipoles to account for the rapid decay of active regions. A 10 gauss field on a scale of 1000 km corresponds to a flux of  $10^{17}$  Mx per dipole. We assume that every granule in the active region carries a new dipole to the surface, and that each dipole is part of a train of dipoles,

connecting the two opposite polarities in the region (cf. Figure 2). The width of an active region, in the direction perpendicular to the line connecting opposite polarities, is typically 50,000 km, and since the width of each bipole is about 1000 km, there are of order 50 trains present at each time. The granular turnover time is about 10 minutes, so that the dipoles can remove flux at a rate of  $5 \cdot 10^7$  Mx/min, or  $7 \cdot 10^{20}$  Mx/day. This is comparable with the decay rate of  $5 \cdot 10^{20}$  Mx/day found by Wallenhorst and Topka (1982).

c) A model involving sub-surface reconnection

To show that our proposed model of flux disappearance is not entirely unreasonable we now consider the possible origin of the dipoles. We suggest they could result quite naturally, if the two opposite polarities of the active region reconnect below the surface, forming a U-shaped magnetic flux tube in the convective zone (see Figure 3). When the lower, horizontal part of this U-loop floats to the surface, it emerges as a series of dipoles, that have an orientation opposite to that of the active region as a whole. The interaction of the dipoles with the overlying horizontal field of the active region leads to a second phase of reconnection, occurring in the chromosphere or low corona. This reconnection process creates small closed-loop structures (Figure 3d), that may be pulled below the solar surface by granules, and may ultimately be destroyed inside the convective zone. In the following we describe this model in more detail.

We suggest that giant-cell convection, occurring in the deep layers of the solar convective zone (Simon and Weiss 1968), is responsible for driving part of the opposite-polarity fields of the active region closer together, thereby forcing the fieldlines to reconnect (cf. Figure 3b). This process could take place in a number of ways. One possibility is that part of the active-region flux remains in the convective updraft that was originally responsible for the formation of the active region. The converging horizontal flows at the base of the updraft push the vertical legs of flux loops toward the center of the updraft region. There turbulent or twisting motions lead to the crossing of flux tubes, resulting in reconnection of opposite polarity fields. This process takes place on the typical timescale of giant-cell convection (about 10 to 30 days). Since the giant cells apparently do not penetrate to the surface (Howard and LaBonte 1980; LaBonte, Howard, and Gilman 1981) the flux tubes are pushed together only in the deeper layers of the convective zone, leading to the formation of a U-loop.

Once a U-loop has formed, the effects of magnetic tension and buoyancy act together in pulling the loop upward. However, the density in the lower, horizontal part of the loop is high, and so it contains a large amount of mass. This mass prevents the U-loop from freely escaping through the solar surface, since gravity will pull the horizontal part back down as soon as it emerges above the photosphere. In order for the U-loop to escape it has to lose its mass. This is difficult in view of the high conductivity of the solar plasma: the magnetic field is nearly "frozen" into the gas. In fact, as long as the flux loop is slender, Ohmic diffusion can only cause a further

increase of the mass in the loop, since pressure equilibrium requires that the gas pressure inside the loop is lower than the external pressure by an amount  $B^2/8\pi$ . Thus, Ohmic diffusion can only drive more mass into the flux loop. It seems clear that U-shaped magnetic loops, floating in the convective zone, cannot simply move out of the sun.

To overcome this difficulty we propose the following scenario for the evolution of a U-loop. As the bottom part of the U-loop rises upward, the density in this horizontal part decreases dramatically. Since the length of the loop, and the mass inside it, remain approximately constant, the cross-sectional area increases. This results in a decrease of the fieldstrength, proportional with the density. We assume that the reconnection occurs at a depth of about 150,000 km below the surface, 50,000 km above the base of the convective zone. When the U-loop rises to a depth of 20,000 km below the surface, just below the layer of supergranules, the density, and therefore the fieldstrength, decrease by a factor 40 (see the convection-zone model of Spruit 1976). If the fieldstrength was of order  $10^4$  Gauss at the reconnection point, then it is only 250 Gauss at 20,000 km, small compared with the local equipartition fieldstrength ( $B_{eq} = 4400$  Gauss). At this point the supergranular flow starts to dominate the motion of the field. We suggest that the supergranules pull stitches of weak field up toward the surface; in Figure 4a we have sketched the topology of the field. Each cell may pull a flux tube of typical size 10,000 km (flux of  $2.5 \cdot 10^{20}$  Mx) out of the underlying horizontal field. This flux does not immediately appear at the solar surface since the fieldstrength is so low: the

convective flow, and not buoyancy, dominates the motion. A small fraction of the flux reaches a depth of about 1000 km below the surface. Since the flux tubes are strongly distorted by supergranulation, gas can flow down to the lowest parts of the fieldlines, and so most of the mass remains at a depth of 20,000 km. Because of these downflows, the fieldstrength at 1000 km depth is difficult to estimate; we suggest it may be on the order of 10 to 100 Gauss. (Note, however, that the fieldstrength would have been much smaller,  $B \approx 0.2$  Gauss, if the field were to remain horizontal all the way up to a depth of 1000 km.)

Then a similar process takes place due to granulation, i.e., on a length-scale of 1000 km. As sketched in Figure 4b, granulation pulls small flux tubes out of the field below, and these tubes emerge at the surface in the form of small dipoles. The flux in each dipole is a few times  $10^{17}$  Mx. The dipoles interact with the overlying coronal field by a reconnection process that occurs at X-type neutral points in the chromosphere or low corona (indicated by crosses in Figure 4b). The reconnection proceeds very rapidly because of the high Alfvén velocity in the chromosphere and corona. The reconnection produces closed flux loops (see Figure 4c). The smaller loops have a typical size of about 1000 km, but some larger ones, that are rooted at about 20,000 km depth and contain most of the mass, also exist. We suggest that the closed loops are subsequently pulled below the surface by the granules. The timescale of emergence, reconnection, and submergence is on the order of the granular turnover time, about 10 minutes. The net effect of the process is the disappearance of field from the surface.

The rate at which the horizontal fields above and below the surface can annihilate each other is determined by the speed at which granulation and supergranulation can transport field to the photosphere. A simple model of this process is that the convection acts as a diffusive medium, which transports a "mean" horizontal field in the vertical direction. The timescale  $\tau$  of the diffusion process is determined by the diffusion constant  $\eta$ , and by the thickness  $d$  of the convecting layer:  $\tau = d^2/\eta$ . Taking  $d = 20,000$  km, and assuming that  $\eta$  is equal to the diffusivity for horizontal motions across the surface ( $D = 200$  km<sup>2</sup>/s, see Sect. 2), we obtain  $\tau = 23$  days. This crude estimate suggests that U-loops can disappear on a timescale of one month.

To summarize, we have suggested that part of the flux in large active regions is reconnected below the surface as a result of the motions within giant cells. The U-loops that are formed in this process float to the surface, and erupt there in the form of small dipoles. The reconnection of these dipoles with the overlying horizontal field in the corona leads to the break-up of the loops into many closed-loop structures. These closed loops contain all the mass of the U-loop, but do not represent any net flux, as seen with low-resolution magnetographs. We conclude that reconnection, first in the deep layers and then again at the surface, may account for the apparently local disappearance of flux.

The final disengagement of mass and magnetic field takes place only by the destruction of the closed loops. This process may involve the contraction of the loops onto themselves, leading to the dissipation of magnetic field at the O-type neutral point at the

center of each loop. The dissipation does not necessarily take place within the photosphere: because of their small size and weak magnetic field, the closed loops may be pulled below the solar surface by the downdrafts at granular boundaries. We suggest that the closed loops contribute to a weak, turbulent magnetic field in the convective zone, that does not represent any "mean" field. This turbulent field has a length scale on the order of the granulation, and may have a typical fieldstrength of a few Gauss. In the course of time the field is dispersed over the sun by convective motions. The inner-network fields observed by Livingston and Harvey (1975) may be a manifestation of the turbulent field.

#### 4. CONCLUSIONS

We have analyzed various observations of flux disappearance, and suggest that active regions disappear more rapidly than can be explained with diffusion models. There is evidence that the flux disappears locally, without any apparent motion towards neutral lines. Such a process cannot be readily explained in terms of the dynamics of surface magnetic fields; it is necessary to invoke rather peculiar processes occurring in the convective zone below. In Sect. 3 we have outlined one particular model, involving the reconnection of fields in the deep layers of the convective zone. Although this model is speculative, it demonstrates that one is forced to consider rather strange processes to explain the phenomenon of "local" flux disappearance.

What are the observational consequences of our model? Of course, high-resolution magnetograph observations should show the presence of small, reverse-polarity dipoles in active regions. To detect these small-scale fields, long time-sequences of magnetograms with sub-arcsecond resolution are required, and the motions of magnetic features on timescales of minutes to days should be followed. Hopefully, the Solar Optical Universal Polarimeter (SOUP) on Spacelab 2 and Sunlab will provide insights into the process. The Coordinated Instrument Package (CIP) on the Solar Optical Telescope will be able to provide us with further data of this type.

Another way in which the process may manifest itself is by the heating of the atmosphere that results from the reconnection of the

bipoles with the overlying coronal field. Unfortunately, it is unclear how much energy may be involved in this process, since only a small fraction of the magnetic energy is dissipated in the atmosphere. Once the field of the U-loops is reconnected, granulation may carry the field down below the surface, where most of the magnetic energy is dissipated.

Finally we note that, in the present paper, we have specifically considered those processes that can affect a single, isolated active region, and we have ignored interactions between active regions. The reason is that enhanced flux-decay seems to be a general phenomena that takes place also in isolated regions, i.e., the interaction with surrounding fields does not seem to be essential. Interactions between active regions may be important, however, in the context of dynamo theory. Parker (1984b), for example, considered active regions erupting on the same toroidal flux tube, and suggested that coronal reconnection of flux from adjacent active regions may lead to the loss of toroidal field from the convective zone. Apart from the scale of the phenomena, Parker's mechanism is similar to ours: the sections of toroidal field in between active regions are like our U-loops, and they may disappear in a similar way. However, in contrast with Parker's model, our U-loops are formed within active regions, and their disappearance does not lead to a loss of toroidal flux.

**Acknowledgements:**

The authors would like to thank Mr. C.R. DeVore and Dr. N.R. Sheeley Jr. for making their results available in advance of publication. We are grateful to Drs. Sheeley, T.D. Tarbell, and C. Zwaan for providing helpful comments on an earlier version of the manuscript. This work was supported by Lockheed's Independent Research program, and by the Air Force Geophysics Laboratory under contract F19628-82-C-6030.

## References:

- Abramowitz, M., and Stegun, I.A. 1964, NBS, Applied Math. Series, Nr. 55
- Beckers, J.M. 1979, Proc. Catania Workshop on Solar Rotation, p.199
- Boris, J.P., Sheeley Jr., N.R., Young, T.R., DeVore, C.R., and Harvey, K.L. 1983. B.A.A.S., 15, 701
- Bumba, V., and Howard, R. 1965, *Astrophys. J.*, 141, 1492
- Duvall, T.L. 1979, *Solar Phys.* 63, 3
- Gaizauskas, V., Harvey, K.L., Harvey, T.W., and Zwaan, C. 1983, *Astrophys. J.*, 265, 1056
- Golub, L., Krieger, A.S., and Vaiana, G.S. 1976, *Solar Phys.*, 50, 311
- Golub, L., Krieger, A.S., Harvey, J.W., and Vaiana, G.S. 1977, *Solar Phys.*, 53, 111
- Golub, L., Davis, J.M., and Krieger, A.S. 1979, *Astrophys. J.*, 229, L145
- Golub, L., Rosner, R., Vaiana, G.S., and Weiss, N.O. 1981. *Astrophys. J.*, 243, 309
- Harvey, K.L., and Harvey, J.W. 1973, *Solar Phys.*, 28, 61
- Howard, R. 1979, *Astrophys. J.* 228, L45
- Howard, R., and LaBonte, B.J. 1980, *Astrophys. J.*, 239, 738
- Howard, R., and LaBonte, B.J. 1981. *Solar Phys.*, 74, 131
- LaBonte, B.J., and Howard, R. 1982, *Solar Phys.*, 80, 361
- LaBonte, B.J., Howard, R., and Gilman, P.A. 1981, *Astrophys. J.*, 250, 796
- Leighton, R.B. 1964, *Astrophys. J.*, 140, 1547
- Livingston, W.C., and Harvey, J.W. 1975, B.A.A.S., 7, 346
- Marsh, K.A. 1978, *Solar Phys.*, 59, 105
- Martin, S.F., and Harvey, K.L. 1979, *Solar Phys.*, 64, 93
- Martin, S.F. 1983, in "Small-scale Dynamical Processes", ed. S. Keil, Sacramento Peak Observatory, New Mexico
- Mosher, J.M. 1977, "The Magnetic History of Solar Active Regions", Ph.D. thesis, California Institute of Technology

- Parker, E.N. 1975, *Astrophys. J.*, 198, 205
- Parker, E.N. 1984a, *Astrophys. J.*, 280, 423
- Parker, E.N. 1984b, *Astrophys. J.*, 281, 839
- Sheeley Jr., N.R. 1969, *Solar Phys.*, 9, 347
- Sheeley Jr., N.R. 1981, in "Solar Active Regions", ed. F.Q. Orrall, Colorado Associated University Press, p. 17
- Sheeley Jr., N.R., Boris, J.P., Young, T.R., DeVore, C.R., and Harvey, K.L. 1983, in "Solar and Stellar Magnetic Fields: Origins and Coronal Effects" (IAU Symp. 102), ed. J.O. Stenflo, p. 273
- Simon, G.W., and Weiss, N.O. 1968, *Z. Astrophys.*, 69, 435
- Spruit, H.C. 1976, Ph.D. thesis, University of Utrecht
- Topka, K., Moore, R., LaBonte, B.J., and Howard, R. 1982, *Solar Phys.* 79, 231
- Van Ballegooijen, A.A. 1982, *Astron. Astrophys.*, 106, 43
- Wallenhorst, S.G., and Howard, R. 1982, *Solar Phys.*, 76, 203
- Wallenhorst, S.G., and Topka, K.P. 1982, *Solar Phys.*, 81, 33
- Zwaan, C. 1978, *Solar Phys.*, 60, 213

**Figure captions:**

**Fig.1.** Vertical cross-section of convective zone, illustrating the disappearance of flux by submergence: (a) two opposite polarity flux tubes move closer together, and (b) are pulled below the surface.

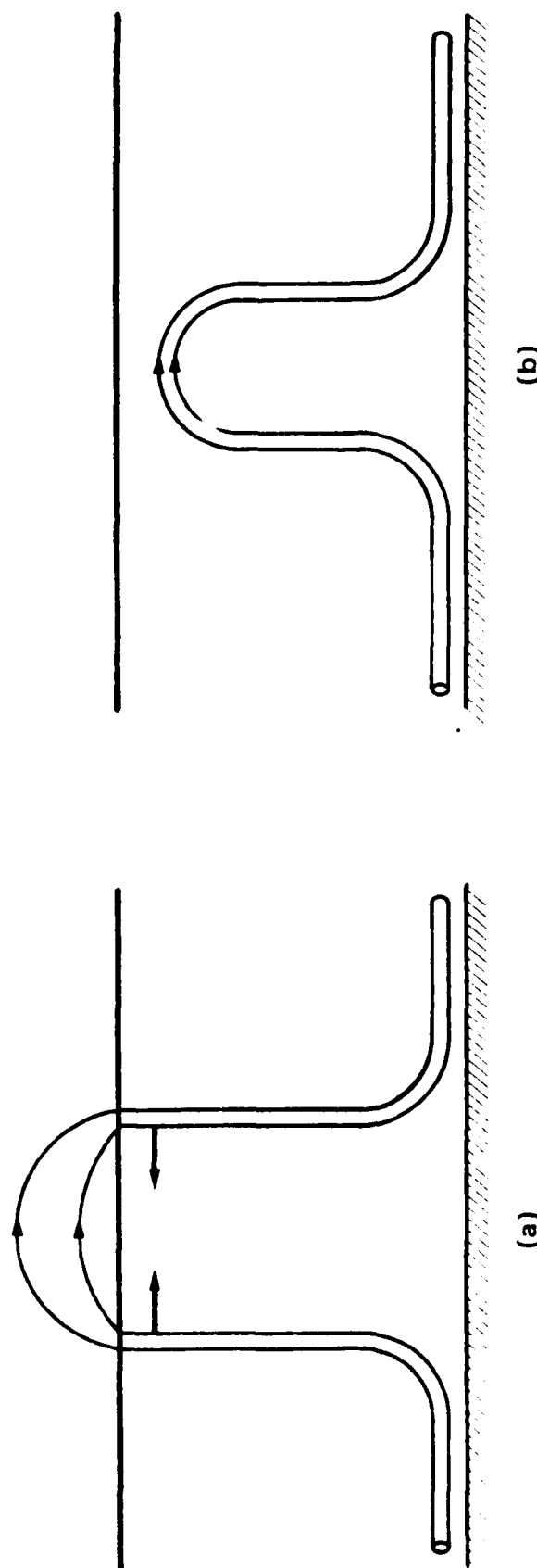
**Fig.2.** The field distribution in the photosphere during the process of flux disappearance: (a) a train of small dipoles erupts in between two patches of opposite polarity; (b) positive (negative) flux elements move a small distance to the left (right), effectively transporting flux over a much larger distance.

**Fig.3.** Illustrating the disappearance of flux by U-loop formation: (a) flux tubes move closer together in the deep layers of the convective zone; (b) reconnection leads to formation of U-loop; (c) horizontal part of U-loop floats up to the surface, and erupts as a series of dipoles; (d) reconnection of dipoles with coronal field produces closed flux loops, which then sink below the surface.

**Fig.4.** The emergence of U-loops: (a) supergranulation distorts the

field, and mass flows to the lowest parts of the loop; (b) granulation brings stitches of field above the surface, where it reconnects with the overlying coronal field (crosses mark X-type neutral points); (c) as a result of reconnection closed loops are formed, that are pulled below the surface while new flux emerges.

Fig. 1



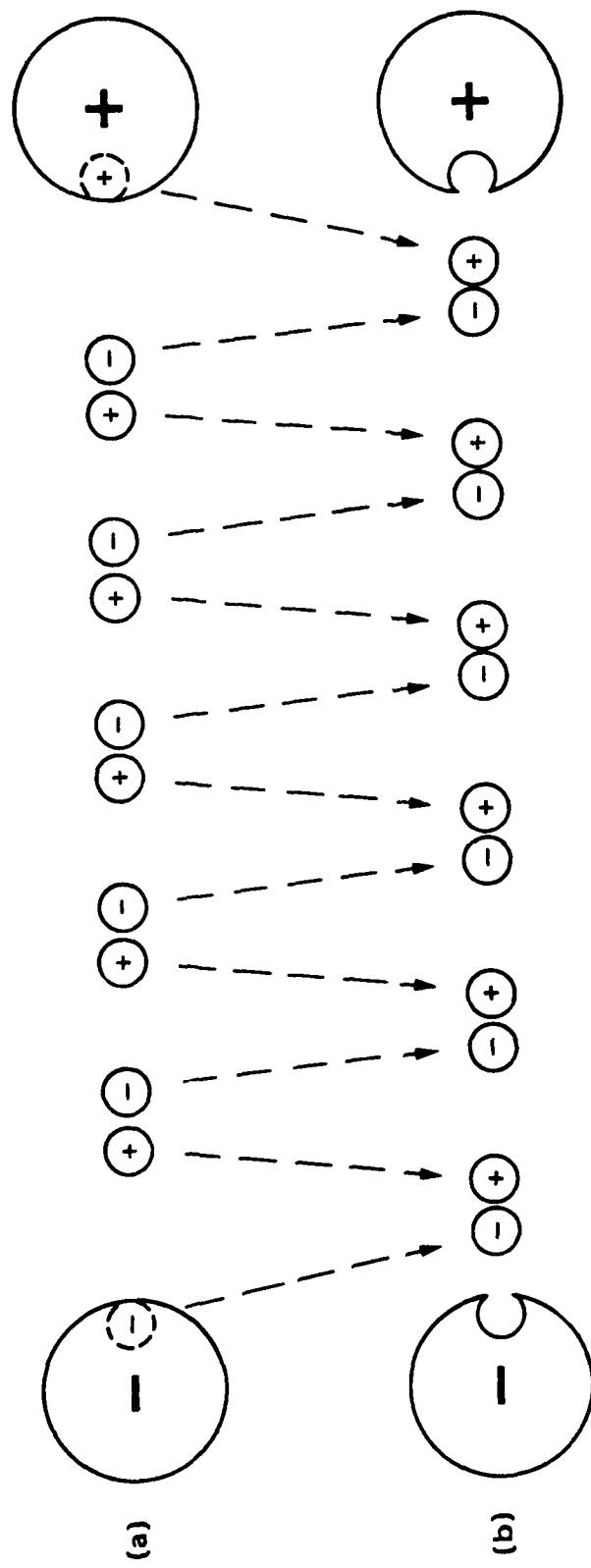
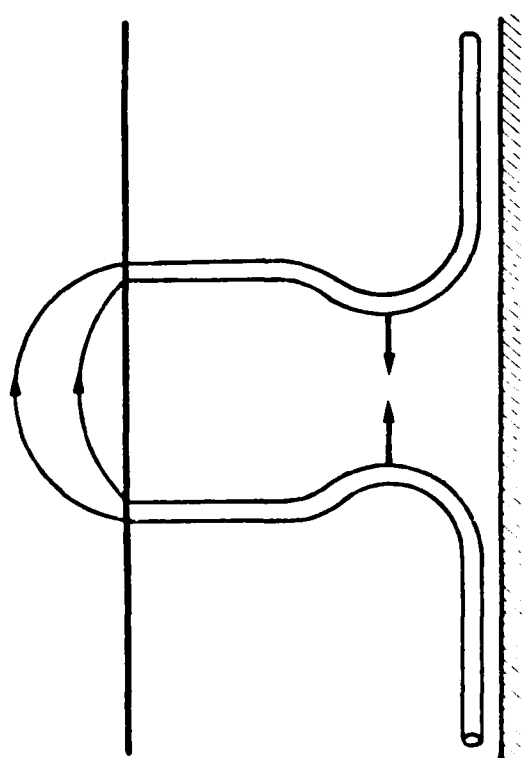
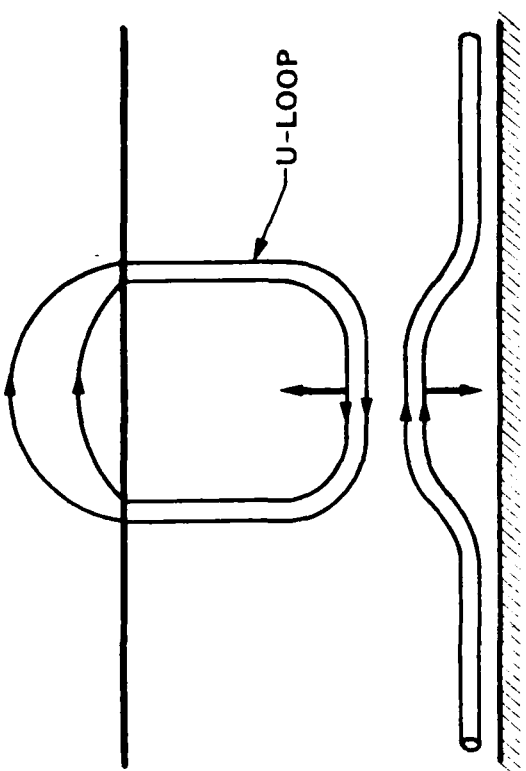


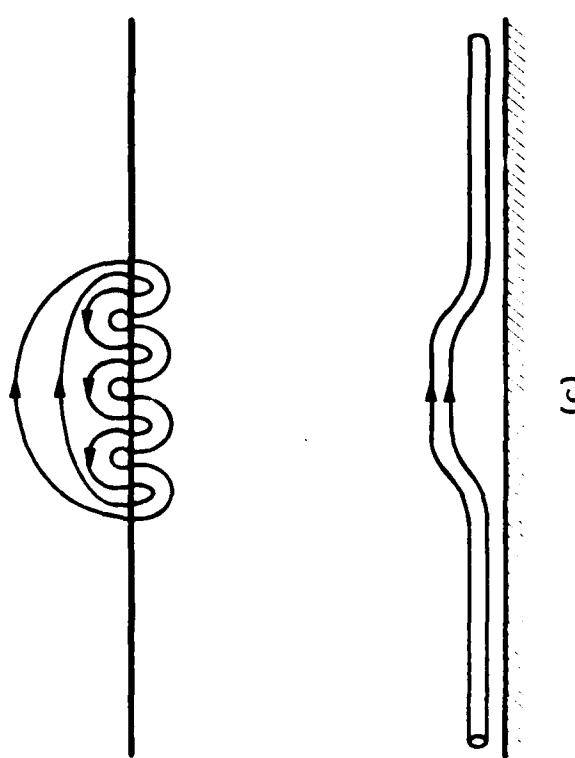
Fig. 2



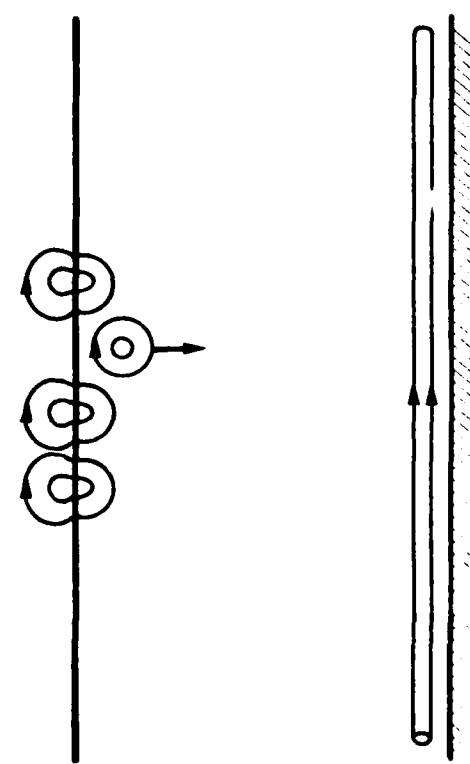
(a)



(b)

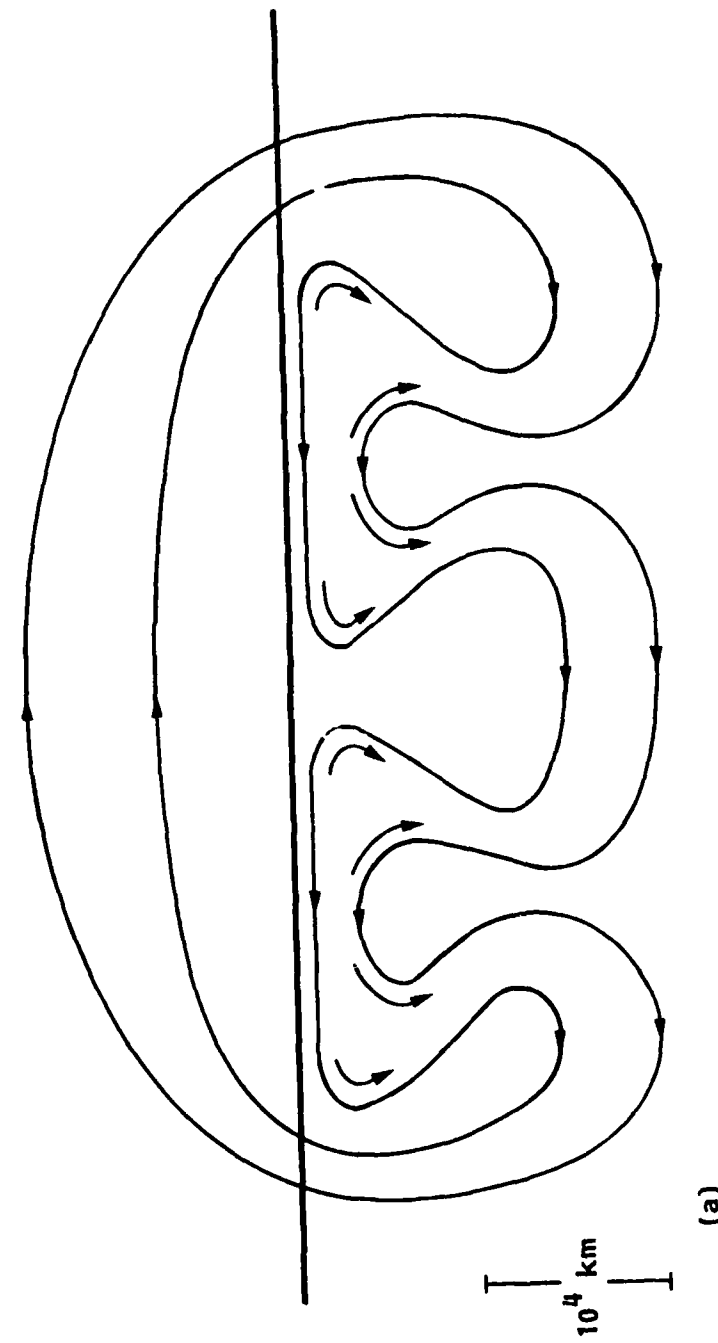


(c)



(d)

Fig. 3



(a)

$10^4$  km

Fig. 4a

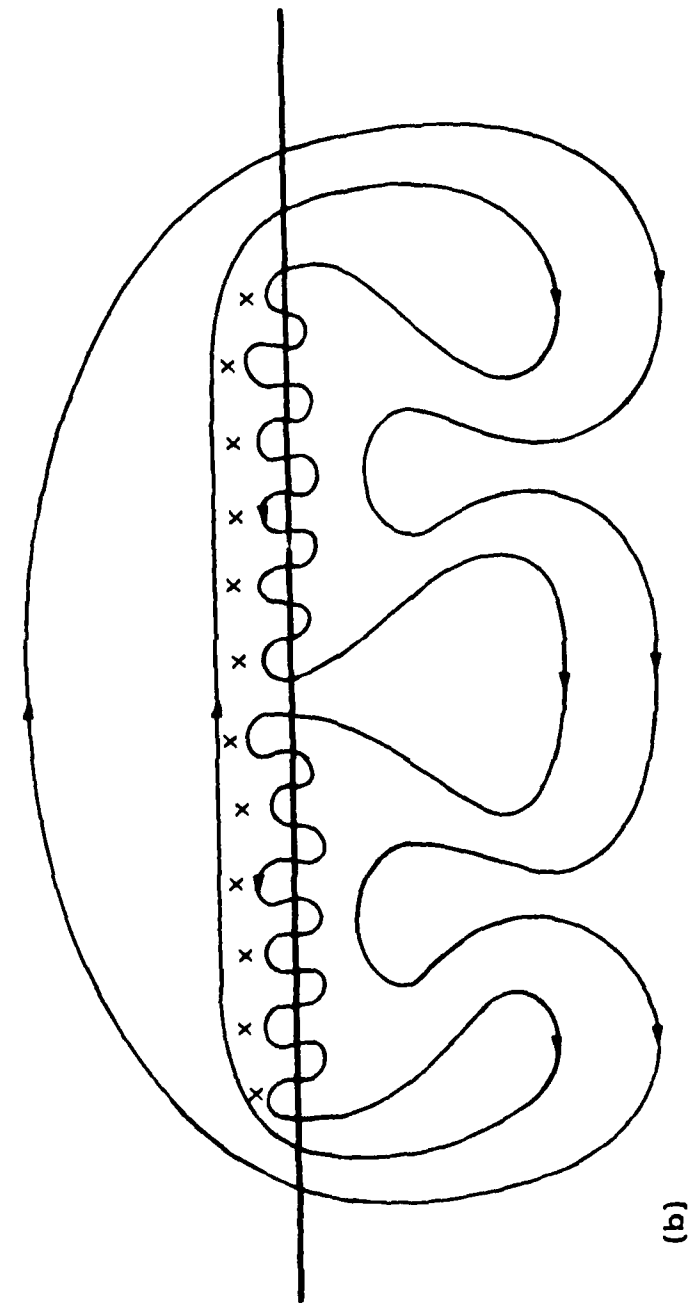


Fig. 4b

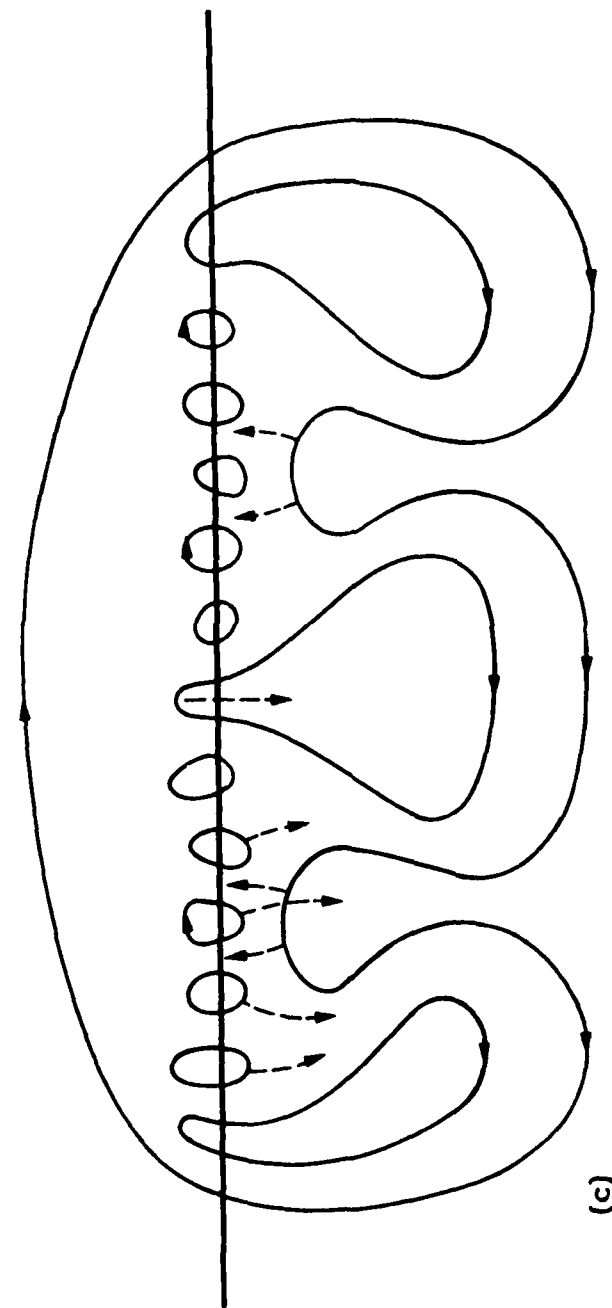


Fig. 4c

**END**

**FILMED**

---

**1-86**

**DTIC**